CHAPTER 4

ABSORPTION, SCATTER, AND CROSS POLARIZATION CAUSED BY PRECIPITATION

4.1 MIE AND RAYLEIGH THEORIES FOR ATTENUATION

Raindrops cause attenuation of radio waves by both absorption and scatter. Absorption involves dissipation of some of the energy of an electromagnetic wave as heat. Scatter involves diversion of some of the energy of the wave into directions other than the forward direction. In the case of a beam of electromagnetic radiation, energy is scattered out of the beam. The term extinction is applied to the sum of absorption and scatter. Attenuation constants can be defined for extinction, absorption, and scatter such that

$$a_{ext} = \alpha_{abs} + a s_{ca} \tag{4.1}$$

where the $a's$ are attenuation constants and can be identified by their subscripts.

Analysis of absorption and scatter by rain drops has often been based upon the assumption of spherical drop shape, but the recent tendency is to take account of the nonspherical form of drops. For drops that are sufficiently small compared to wavelength, Rayleigh theory applies, but for drops that have sizes comparable to wavelength the more complicated Mie theory, or refinements of it, must be used. Drops with radii ≤ 170 μm are essentially spherical, whereas drops with radii betweem 170 and 500 μm are closely approximated by oblate spheroids. (An oblate spheroid is formed by rotating an ellipse about its shortest axis.) Between 500 and 2000 μm, drops are deformed into asymmetric oblate spheroids with increasingly flat bases, and drops ≥ 2000 μm develop a concave depression in the base which is more pronounced for the largest drop sizes (Pruppacher and Pitter, 1971). The ratio of the minor to major axes of oblate spheroid drops is equal to 1 - a, where a is the radius in cm of a spherical drop having the same volume. Figure 4.1 shows an example of the shape of a very large drop.

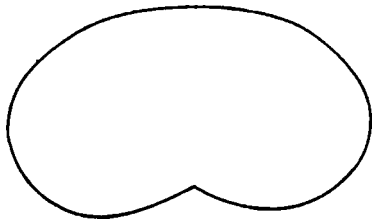

Figure 4.1. Form of a very large raindrop (Pruppacher and Pitter, 1971).

The total or extinction power-density attenuation constant a_p for rain can be expressed as

$$\alpha_p = \int_a N(a)\ C_{ext}\left(n_c, a/\lambda_o\right) da \qquad (4.2)$$

where a summation is indicated over all drop radii a, n_c is the complex index of refraction of water which is a function of temperature and frequency, and λ_o is wavelength in air. C_{ext} is an extinction coefficient and is shown as being expressed as a function of n_c and a/λ_o. N(a) da represents the number of drops per cubic meter in the size interval da and is determined by the drop size distribution which is a function of rain rate. [N(a) has units of m^{-4}, and N(a) da has units of m^{-3}.] *Distributions of drop sizes have been determined empirically, the most widely used and tested distribution being the Laws and Parsons (1943) distribution. The Marshall and Palmer (1948) distribution is also well known, The Laws and Parsons data (Table 4.1) obtained by collecting rain drops in pans of flour do not provide N(a) da, but M(a) da, the fraction of the total volume of water striking the ground due to drops of a given size. To determine N(a) da, one must use M(a) da and alsc v(a), the limiting terminal velocity of raindrops as a function of size, in

$$N(a)\,da = \frac{M(a)\,da\,R}{v(a)\,a^3\,15.1} \qquad (4.3)$$

Here R is rain rate in mm/h, v(a) is in m/s, a is in cm, M(a) is nondimensional, and N(a) da is in m^{-3}. The Laws and Parsons data are obtained for a finite, rather than infinitesimal. value of da of 0.025 cm, and Eq. (4.2) is thus evaluated in' practice as a summation instead of an integral. Values of v(a) are given in Fig, 4.2.

The Marshall and Palmer distribution, made by making measurements on dyed filter papers, has the form of

$$N(R,a) = No\ e^{-ca} \qquad (4.4)$$

where R is rain rate and a is drop radius. N and No are sometimes stated in units of cm^{-4}, corresponding to the number of drops per cm^3 in a size range of one cm in radius. In these units No has the value of 0.16. If a is in cm and R is in mm/h

$$c = 82\ R^{-0.21} \qquad (4.5)$$

The number of drops in a volume V, in units of cm^3, having radii between a and a + da is given by N da V. The Laws and Parsons distribution can also be approximated by an equation of the form of Eq. (4.4).

The determination of C_{ext} has been commonly based on the Mie theory for spherical drops (Kerr, 195 1; Kerker, 1969; Zufferey, 1972). In this case C_{ext} has the form of

$$C_{ext}\left[n_c,\ a/\lambda_o\right] = (\lambda_o^2/2)\ \mathrm{Re} \sum_{n=1}^{\infty} (2n + 1)\ (a_n + b_n) \qquad (4.6)$$

where λ_o is wavelength in air and an and b_n are coefficients involving spherical Bessel and Hankel functions of complex arguments. C_{ext} and So, which gives the amplitude of the forward scattered wave, are related by

Table 4.1 Laws and Parsons Distribution Giving the Percent of Volume Reaching Ground Contributed by Drops of Various Sizes, *

Drop Radius a (mm)	Rain Rate (mm/h) 0.25	1.25	2.5	1.2.5	25	50	100	150
0-0.125	1.0	0.5	0.3	0.1				
0.125-0.375	27.0	10.4	7.0	2.5	1.7	1.2	1.0	1.0
0.375-0.625	50.1	37.1	27.8	11.5	7.6	5.4	4.6	4.1
0.625-0.875	18.2	31.3	32.8	24.5	18.4	12.5	8.8	7.6
0.875-1.125	3.0	13.5	19.0	25.4	23.9	19.9	13.9	11.7
1.125-1.375	O*7	4.9	7.9	17.3	19.9	20.9	17.1	13.9
1.376-1.625		1.5	3.3	10.1	12.8	15.6	18.4	17.7
1.625-1.875		0.6	1.1	4.3	8.2	10.9	15.0	16.0
1.875-2.125		0.2	0.6	2.3	3.5	6.7	9.0	11.9
2.125-2.375			0.2	1.2	2.1	3.3	6.8	7.7
2.375-2.625				0.6	1.1	1.8	3.0	3.6
2.625-2.875				0.2	0.5	1.1	1.7	2.2
2.875-3.125					0.3	0.5	1.0	1.2
3.125-3.375						0.2	0.7	1.0

*Drop radius interval, da = 0.25 mm. Multiply percents g values by 0.01 to obtain M(a) da, e.g. for 50 mm/h and i. 125-1375 mm, M(a) da = 0.209.

After J.O. Laws and D.A. Parsons, "The relation of drop size to intensity," Trans. of the A. Geophysical Union, pp. 452-46 , 1943.

$$c_{ext}\left(n_c, a/\lambda_o\right) = (4\pi/\beta_o^2)\,\mathrm{Re}\;\mathrm{So}\;\left[n_c,\ a/A_0\right]_1 \qquad (4.7)$$

where β_o is the phase constant $2\pi/\lambda_o$.

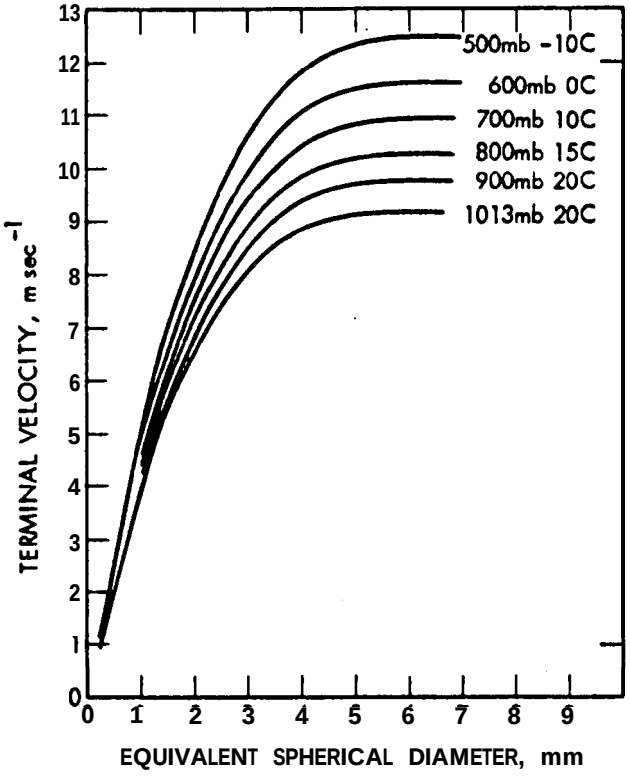

Figure 4.2 Terminal velocity of raindrops at six pressure levels in a summer atmosphere as a function of equivalent spherical diameter. (From Beard, "Terminal velocity and shape of cloud and precipitation drops aloft," J. of Atmospheric Sciences, May 1976.) The pressures 1013, 900, 800, 700, 600, and 500 mb correspond roughly to altitudes of O, 0.98, 1.95, 3.0, 4.2, and 5.6 km respectively of the U.S. Standard Atmosphere, 1976.

For frequencies of about 3 GHz and less, the Rayleigh approximation can be used instead of the Mie theory. For this case C_{ext} takes the form of

$$C_{ext} = (4\pi^2 a^3/\lambda_o)\, 6K_i/[(K_r + 2)^2 + K_i^2] \qquad (4.8)$$

where K_i is the imaginary part of relative dielectric constant of water and K_r is the real part. The complex index of refraction n_c and complex relative dielectric constant Kc are related by $n_c^2 = K_c$.

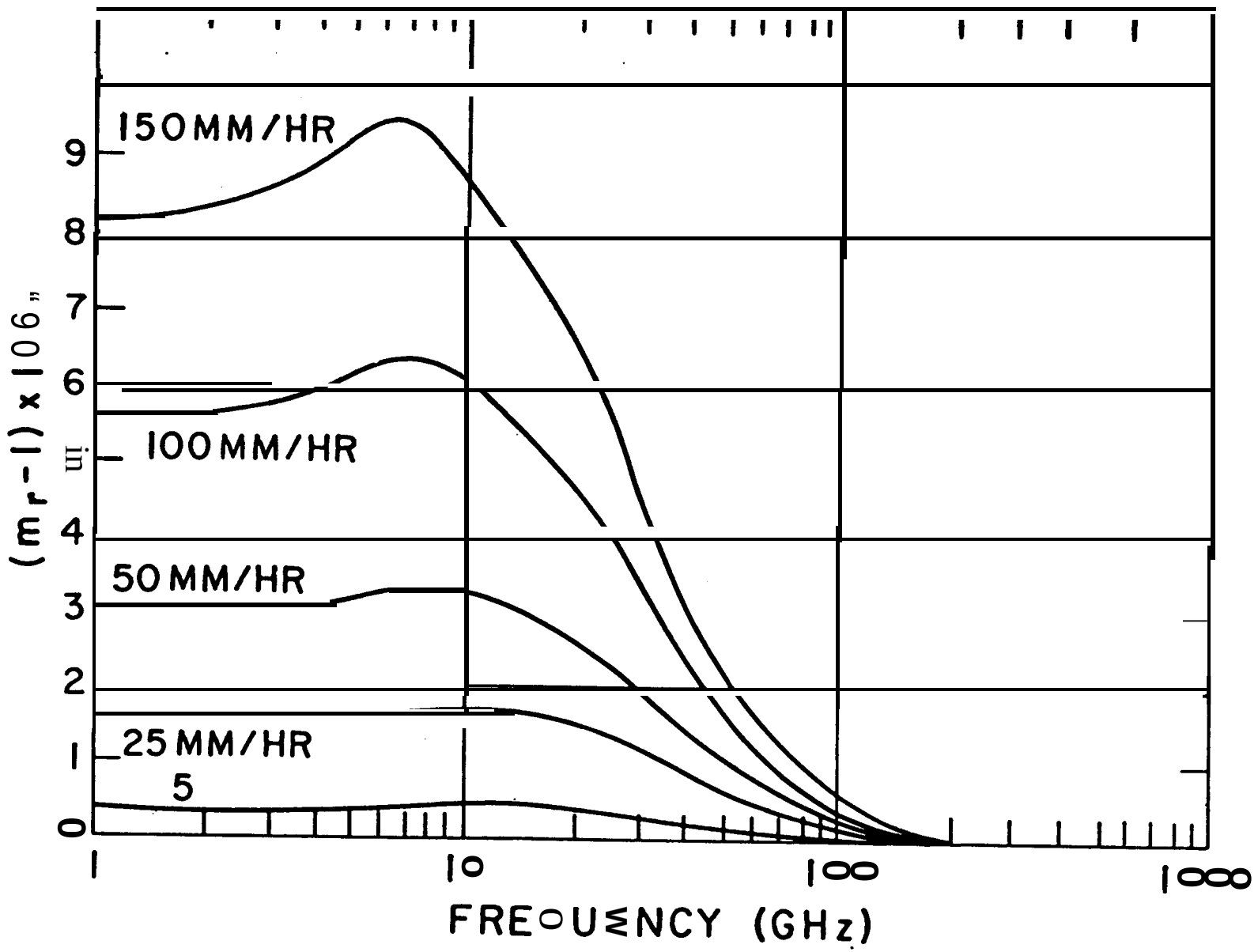

Figure 4.3a. The real part minus unity times 10^6 of the complex index of refraction of rain at 20 deg C (Zufferey, 1972).

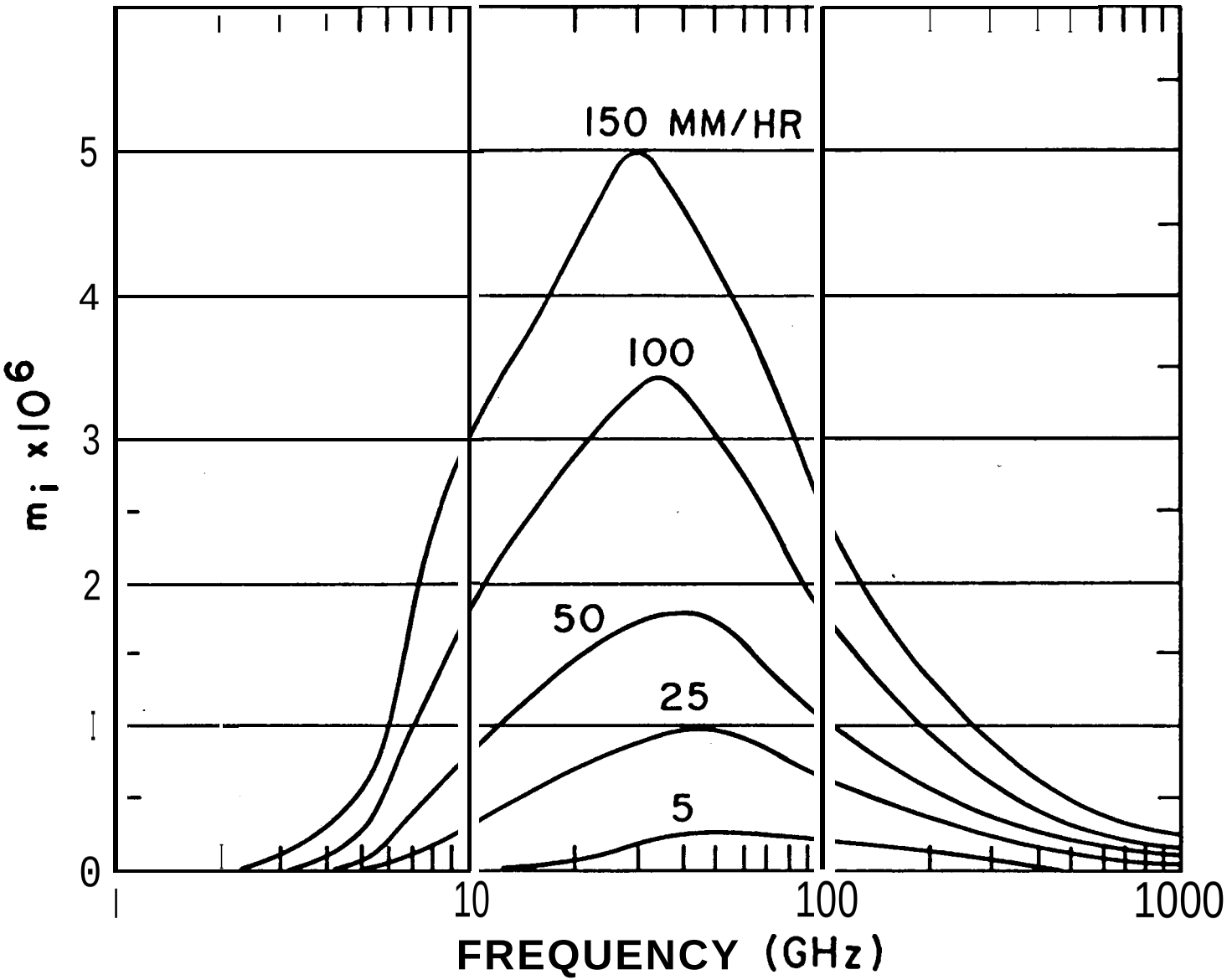

Figure 4.3b. The imaginary part times 10^6 of the complex index of refraction of rain at 20 deg C (Zufferey, 1972).

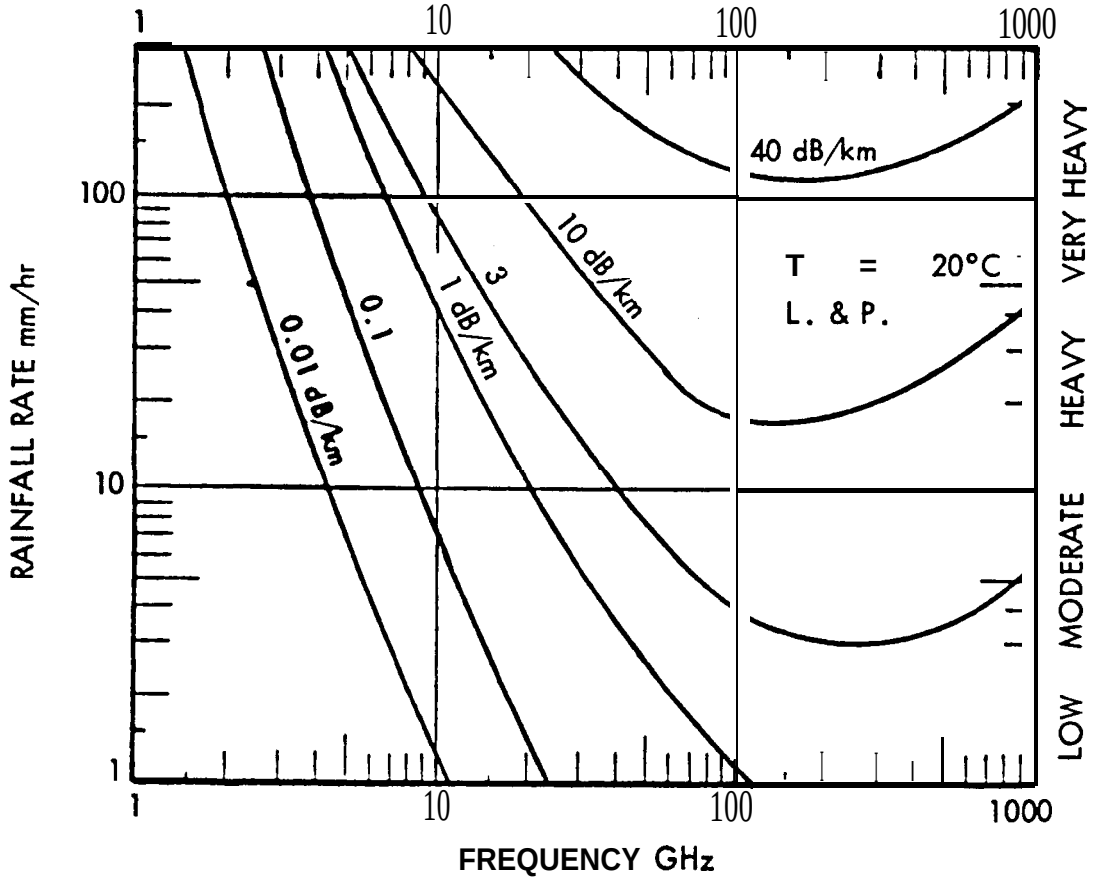

Figure 4.4. Rain rate versus frequency for specific values of attenuation constant (Zufferey, 1972).

An alternative procedure for determining the attenuation constant involves calculating an effective complex index of refraction m_c for the medium in terms of So by use of

$$m_c - 1 = j\,(2\pi/\beta_o^3) \int_a N(a)\, S_o \left[n_c, a/\lambda_o\right] \quad (4.9)$$

This approach has been described by van de Hulst (1957) and Kerker (1969) but early consideration of the concept is attributed by Kerker to an 1899 paper by Rayleigh and 1890 and 1898 papers by Lorenz. The medium in question consists of water drops in empty space. The imaginary part m_i of the complex index m_c determines the field intensity attenuation constant α by use of

$$\alpha = \beta_o\, m_i \quad \text{Nepers/m} \quad (4.10)$$

The power density attenuation constant α_p is related to the field intensity constant by $\alpha_p = 2\,\alpha$. To obtain attenuation in dB/m multiply α by 8.68 or α_p by 4.34. The phase constant β for the medium can be obtained from $\beta = \beta_o\, m_r$.

Values of the real part minus one and the imaginary part of the complex index m_c are shown in Figs. 4.3a and 4.3b. Plots of rain rate versus frequency for specific values of the attenuation constant are given in Fig. 4.4. These curves show that attenuation increases with rain rate up to about 100 GHz or more.

4.2 EMPIRICAL RELATIONS BETWEEN RAIN RATE AND ATTENUATION

Empirical relations between rain rate and attenuation constant have been developed and are widely used for practical application. In the remainder of this chapter the empirical relations will be primarily what is used to estimate attenuation due to rain. These relations have the form of

$$\alpha_p = a(f)\, R^{b(f)} \quad (4.11)$$

where a and b represent values which are a function of frequency f and R is rain rate in mm/h. The first observation of a relation of this type, but with b = 1, is credited to Ryde (1 946). Values of a(f) and b(f) have since been determined by several workers including Zufferey (1972) who gave sets of values for light and heavy rain, the dividing line being taken as 10 mm/h. Olsen, Rogers, and Hedge (1978) have analyzed the relation thoroughly and derived tables of values of a(f) and b(f) for the Laws and Parsons and Marshall-Palmer distributions and for the drizzle and thunderstorm distributions of Joss. Their tables include the range from 1 to 1000 GHz for temperatures of O, 20, and -10 degC. Values based on the Laws and Parsons distribution for frequencies of 15 GHz and lower for O deg C are given in Table 4.2. The values LP_L apply for low rain rates, and LP_H values are for high rates, with some overlap. We take 30mm/hto be a suitable dividing line and assume that either set of values can be used for that rate. Figure 4.5 shows values of attenuation constant as given in CCIR Report 721-2 (CCIR, 1986a). In addition estimates of the attenuation constant for frequencies below 10 GHz can be taken from Fig. 4.4. For frequencies of 3 GHz or less values of the attenuation constant can be calculated by using Eq. (4.8) for C_{ext}.

The widely used constants provided by Olsen, Rogers, and Hedge (1978) apply to spherical drops for which attenuation is independent of wave polarization. Attenuation for spheroidal drops depends on wave polarization, and Table 4.3 gives values of the constants a and b for vertical and horizontal polarization. Values for arbitrary polarization, including circular, can be derived from those for vertical and horizontal polarization by use of

$$a = [a_H + a_V + (a_H - a_v)\cos^2\theta \cos 2\tau\ ]/2 \qquad (4.12)$$

$$b = [a_H b_H + a_V b_V + (a_H b_H - a_V b_V)\cos^2\theta \cos 2\tau\ ]/2a \qquad (4.13)$$

The subscripts H and V refer to horizontal and vertical polarization. The angle θ is the elevation angle of the path, and τ is the tilt angle of the electric field intensity vector from the horizontal. The angle τ can be taken to be 45 deg for circular polarization. Values for frequencies intermediate , between those of Table 4.3 can be obtained by interpolation. Now that information is available to determine a and b for arbitrary polarization, it seems advisable to

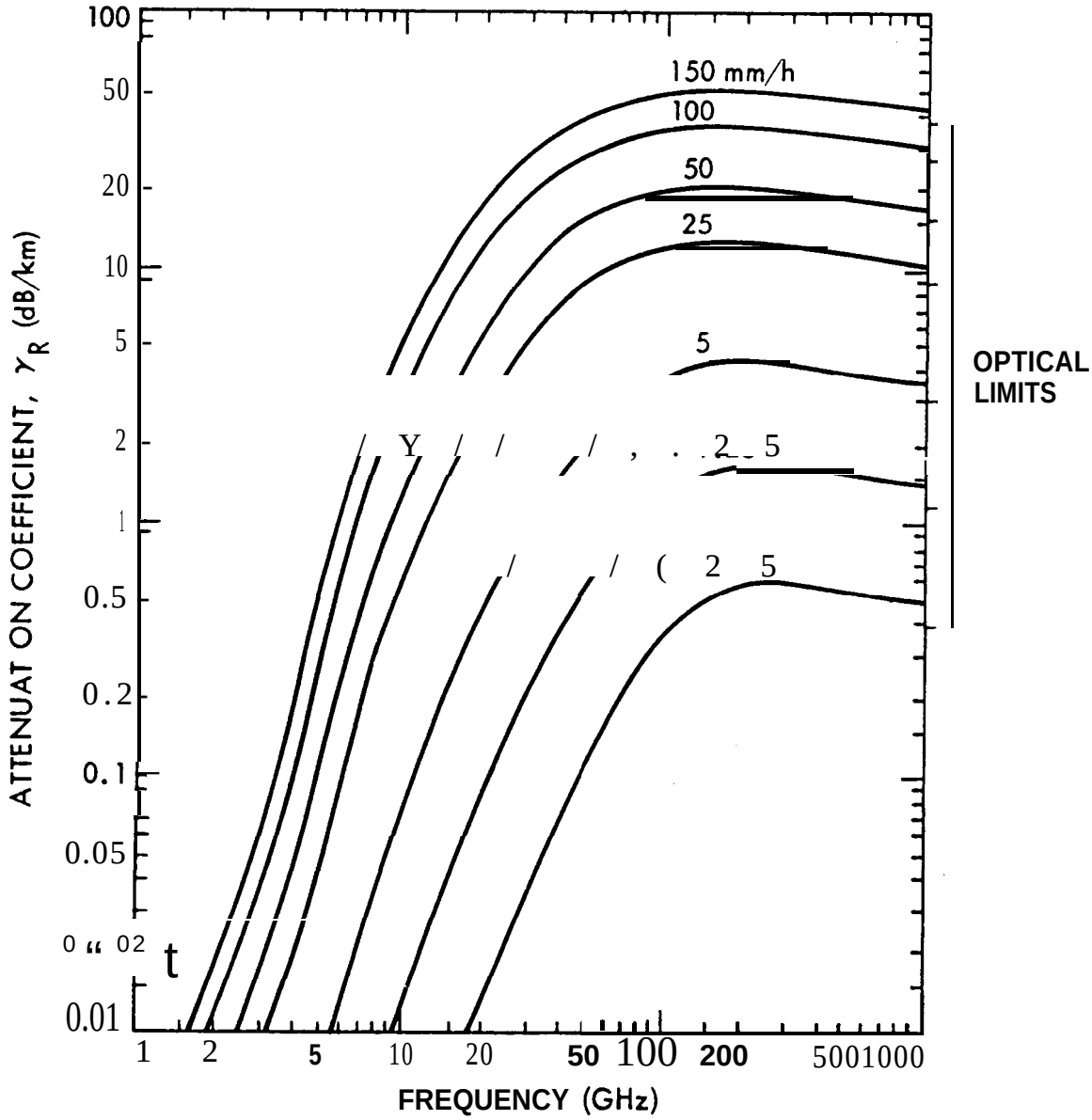

Figure 4.5, Attenuation constant as a function of rain rate and frequency (CCIR, 1986a),

Table 4.2 Values of a and b of Eq. (4.11) from Olsen, Rogers, and Hedge (1978) for T = 0 deg for High and Low Rain Rates.

Freq. (GHz)	a		b	
	LP_L	LP_H	LP_L	LP_H
1.0	6.41×10^{-5}	5.26×10^{-5}	0.891	0.947
1.5	1.45×10^{-4}	1.14×10^{-4}	0.908	0.976
2.0	2.61×10^{-4}	1.96×10^{-4}	0.930	1.012
2.5	4.16×10^{-4}	2.96×10^{-4}	0.955	1.054
3.0	6.15×10^{-4}	4.12×10^{-4}	0.984	1.100
3.5	8.61×10^{-4}	6.42×10^{-4}	1.015	1.150
4.0	1.16×10^{-3}	6.84×10^{-4}	1.049	1.202
5.0	1.94×10^{-3}	1.12×10^{-3}	1.113	1.274
6.0	3.05×10^{-3}	1.99×10^{-3}	1.158	1.285
7.0	4.55×10^{-3}	3.36×10^{-3}	1.180	1.270
8.0	6.49×10^{-3}	5.35×10^{-3}	1.187	1.245
9.0	8.88×10^{-3}	8.03×10^{-3}	1.185	1.216
10	1.17×10^{-2}	1.14×10^{-2}	1.178	1.189
11	1.50×10^{-2}	1.52×10^{-2}	1.171	1.167
12	1.86×10^{-2}	1.96×10^{-2}	1.162	1.150
15	3.21×10^{-2}	3.47×10^{-2}	1.142	1.119

Table 4.3 The Coefficients a and b for Calculating Attenuation for Horizontal and Vertical Polarization (CCIR, 1986a).

Frequency (GHz)	a_H	a_v	b_H	b_v
1	0.0000387	0.0000352	0.912	0.880
2	0.000154	0.000138	0.963	0.923
4	0.000650	0.000591	1.12	1.07
6	0.00175	0.00155	1.31	1.27
8	0.00454	0.00395	1.33	1.31
10	0.0101	0.00887	1.28	1.26
12	0.0188	0.0168	1.22	1.20
15	0.0367	0.0347	1.15	1013

obtained by interpolation. Now that information is available to determine a and b for arbitrary polarization, it seems advisable to use that information. Values of the well established and somewhat more detailed tables of Olsen, Rogers, and Hedge (1978) are nevertheless included for completeness.

Interest in attenuation due to rain tends to be concentrated at the higher frequencies above 10 GHz where attenuation is the greatest, but the plots of Figs. 4.4 and 4.5 extend below 10 GHz as well. The values from the two figures are in general agreement, both showing that for frequencies of 10 GHz or less and rainfall rates of 100 mm/h or less, the attenuation constant has a value of about 3 dB/km or less. Attenuation constants of this order of magnitude, while less than for high- frequencies, may still be serious, and concern about attenuation due to rain is thus not confined to the higher frequencies but includes all of the X band (8-12 GHz). Attenuation due to rain increases the loss factor L in relations determining the signal-to-noise ratio (Sec. 1.1). It should be kept in mind also that 'rain increases the systems noise temperature, T_{sys}, as well (Chap.7).

4.3 STATISTICAL ANALYSIS OF ATTENUATION DUE TO RAIN

Procedures for calculating the attenuation constant for propagation through rain as a function of rain rate were described in Sees. 4.1 and 4.2. For predicting the attenuation expected on an earth-space path, one also needs to have a statistical model for the point rainfall intensity at locations or in regions of interest. In particular one generally needs to have an estimate of the rainfall rates that are exceeded for certain small percentages of time. Methods for obtaining rainfall data are described in Sec. 4.3.1. A third need is for a model of the spatial distribution of rainfall, as a function of height and distance from the station, and this topic is treated in Sec. 4.3.2. Finally several models that have been developed for widespread application, in some cases for worldwide use, are described in Sec. 4.3.3.

4.3.1 Rainfall Data

A first step in developing an understanding of the effect of rain on propagation in a particular area may be to obtain raw data on the occurrence of rain there. When sufficient raw data have been accumulated, it canbe put into statistical form.

Published data on rain are already available for the United States from the National Climatic Center (Asheville, North Carolina 2880 1) of the National Weather Service. They supply Hourly Precipitation Data, issued monthly by state (including monthly maximum rainfalls for periods for as short as 15 min for a number of stations in each state); Climatologial Data, issued monthly by state (includes daily precipitation amounts); Climatological Data-National Summary, issued monthly (includes monthly rainfall and greatest rainfall in 24 h); Climatological Data - Annual Summary (includes maximum rainfalls in periods ranging from 5 to 180 minutes); Local Climatological Data, issued monthly (includes hourly rainfall for individual weather stations); and Storm Data, published monthly for the United States, In Canada Monthly Records for Western Canada, Northern Canada, and Eastern Canada and a monthly Canadian Weather Review are available from Supply and Services Canada, Publishing Centre (Hull, Quebec KDA0S9). Data for a number of other countries are on file at the National Weather Service Library, Room 816, Gramax Bldg., 13th Street, Silver Spring, MD.

Rain guges are the means used for obtaining most of the National Weather Service rain data. A common type of gauge is supported in a vertical position and has a receiving area ten times the cross section of the measuring tube to facilitate precision in measurement. The amount of precipitation is determined by use of a hardwood measuring stick. Automatic tipping-bucket and universal weighing gauges are in use at National Weather Service stations that are manned by their own personnel (First Order Weather Stations), and chart records from these gauges can be obtained form the National Climatic Center.

If it is deemed advisable to obtain additional data on rainfall or attenuation caused by rain because of lack of detailed published data, a variety of options can be followed if sufficient financial support and manpower are available. One can set up rain gauges of the

tipping bucket or weighing type. Radar can monitor precipitation over a wide area using the concepts discussed in Sec. 4.5 for bistatic scatter. For monostatic radar the distances R_1 and R_2 are the same, however, and the scattering volume V is proportional to R^2 for widespread rain, so the ratio of W_R/W_T (received power to transmitted power) is proportional R^{-2} as shown in Eq. (4. 14).

$$W_R/W_T = \frac{G^2\,\theta_{HP}\,\phi_{HP}\,c\,\tau\,\pi^3}{1024\,(\ln 2)\,R^2\lambda^2}\left|\frac{K_c - 1}{K_c + 2}\right|^2 z \qquad (4.14)$$

The quantity G is radar antenna gain, θ_{HP} and ϕ_{HP} are the half-power beamwidths of the radar antenna, c is about 3 x 108 m/s, r is the radar pulse length, λ is wavelength, and Kc is the complex relative dielectric constant of water. Z represents $\sum d^6$ where d is drop diameter and is related to the rain rate R by $Z = 400\,R^{1.4}$ for the Laws and Parsons distribution and $Z = 200\,R^{1.6}$ for the Marshall and Palmer distribution. Equation (4. 14) thus allows determining the parameter Z which in turn allows estimating the rain rate R on the basis of the empirical relations given.

Another approach to measuring attenuation due to rain on earth-space paths is to use radiometer techniques. One procedure of this type involves using the Sun as a source. When a source hang an effective temperature Ts is viewed through an absorbing medium having an effective temperature of T_i, the observed brightness temperature T_b is given by (Sec. 7.2)

$$T_b = T_s\,e^{-\tau} + T_i(1 - e^{-\tau}) \qquad (4.15)$$

where τ is referred to as optical depth and is the integral of the the power-density attenuation coefficient along the path, namely $\int \alpha_p\,dl$. The temperatures of Eq. (4. 15) are measures of power, as kT_bB where k is Boltzmann's constant and B is bandwidth, is power. The first term on the right-hand side of Eq. (4.15) represents the power from the Sun attenuated by the Earth's atmosphere and the second term represents thermal noise emitted by the Earth's atmosphere.

The Sun subtends an angle of 0.5 deg viewed from the Earth, and if the antenna of the radiometer is perfectly aligned with the Sun and the Sun fills the beam, Ts is the effective brightness temperature of the Sun. Otherwise T_s is the average brightness temperature within the antenna beamwidth, as determined by the temperature of the Sun itself and the low background level of about 2.7 K. The object of using Eq. (4.15) is to determine τ due to rain, This can be accomplished by first using the Sun as a source and then switching away from the Sun, The difference between the two values of T_b is $T_s e^{-\tau}$ and if Ts is known then τ is known. Ts can be determined by using the Sun as a source when no rain is present.

If the value of T_i of Eq. (4. 15) is known then it is not necessary to use the Sun as a source. Instead one can point away from the Sun and record

$$T_b = T_i (1 - e^{-\tau}) \qquad (4.16)$$

from which τ and the corresponding attenuation in dB ($A_{dB} = 4.34 \tau$) can be determined. T_i can be determined originally from measurements using the Sun or in some other way. It tends to be less than the physical temperature where rain is falling because total attenuation is due to scattering as well as absorption. It is only when attenuation is due to absorption alone that T_i can be expected to be equal to actual temperature.

A large amount of data on attenuation due to rain, much of it collected by. using beacons on satellites, has been accumulated. The CCIR has established a data bank for earth-space propagation that includes data on rain attenuation (CCIR, 1983a; Crane, 1985a). NASA has sponsored an extensive study program on attenuation due to rain (Kaul, Rogers, and Bremer, 1977; Ippolito, 19'78). The Nov.-Dec. 1982 issue of Radio Science was devoted to NASA sponsored propagation studies, including those about rain. Many of the studies' of' rain have been directed at frequencies above 10 GHz, but a considerable amount involves frequencies not far above (Arnold, Cox, and Rustako, 198 1; Nackoney and Davidson, 1982; Vogel, 1982; Bostian, Pratt, and Stutzman, 1 '986).

4.3,2 Spatial Distribution of Rainfall

1. Vertical Distribution: Temperature decreases with height and precipitation tends to occur as snow rather than rain above the O deg C isotherm. Snow causes considerably less attenuation than rain, and it is the length of the path up to the O deg C isotherm that largely determines attenuation due to precipitation. Modeling the spatial distribution of rain is difficult and several procedures have been proposed for determining the height extent H of rainfall for estimating attenuation. Figure 4.6 shows curves for what were designated in 1 983 as Methods 1 and 2 and also a lower dotted modification of Method 1 for latitudes below 40 deg (CCIR, 1983b). The modification was suggested by parties that thought that the other curves resulted in attenuation values that were excessively high for these latitudes. Method 1, including the dotted modification, and Method 2 have both been replaced, however, and the latest recommended CCIR procedure (CCIR, 1986b,c) is to use the relation given here as Eq. (4.30). This relation is based on 1984 Report 352 of the University of Bradford by Leitao, Watson, and Brussaard, prepared for the European Space Agency. See No. 8 of Sec. 4.3.3 for further discussion of the CCIR models.

2. Horizontal Distribution: Intense rain tends to be localized, and, especially when one is concerned with the high rain rates that are exceeded for small percentages of time, a procedure is needed to account for the fact that high rain rates will very likely not occur along the total length of the path. Some approaches involve determining an effective path length or path reduction factor. The original version of the Global Model (CCIR, 1978) used a path reduction factor $r = \gamma(D)\, R^{-\delta(D)}$ where D is horizontal extent of the path through rain and R is rain rate. This factor is shown graphically in Fig. 4.7. The 1982 CCIR model involves determination of a path reduction factor in an especially simple manner, and this approach has been retained in the latest . CCIR report on the subject (CCIR, 1986b). While questions may be raised about this procedure, its simplicity is an advantage. In other cases, an effort is made to model the rain rate that can be expected along the path and to calculate the attenuation accordingly

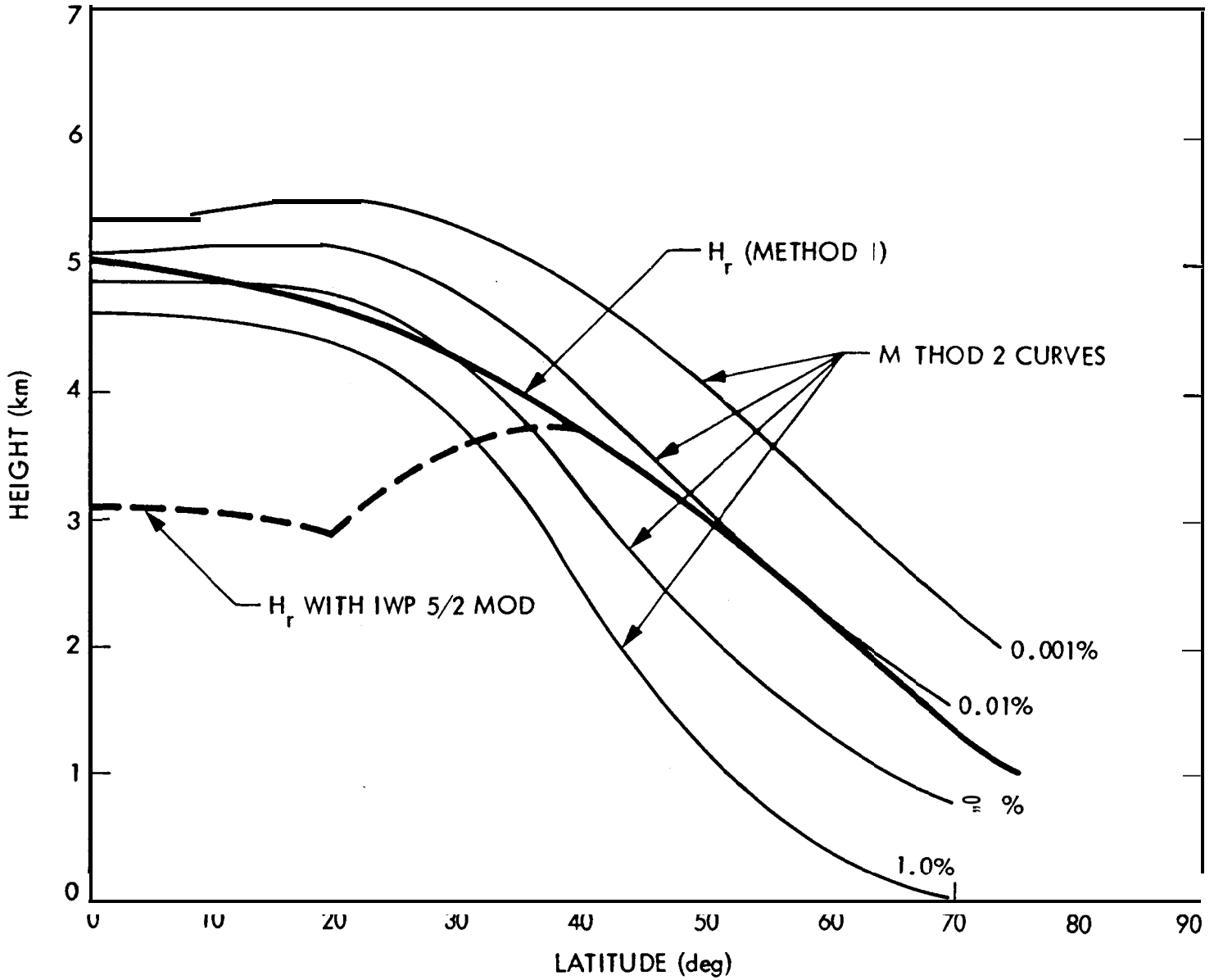

Figure 4.6. Heights of 0 deg C isotherms for Methods 1 and 2 (CCIR, 1983b). The latest recommended procedure, however, utilizes Eq. (4.30).

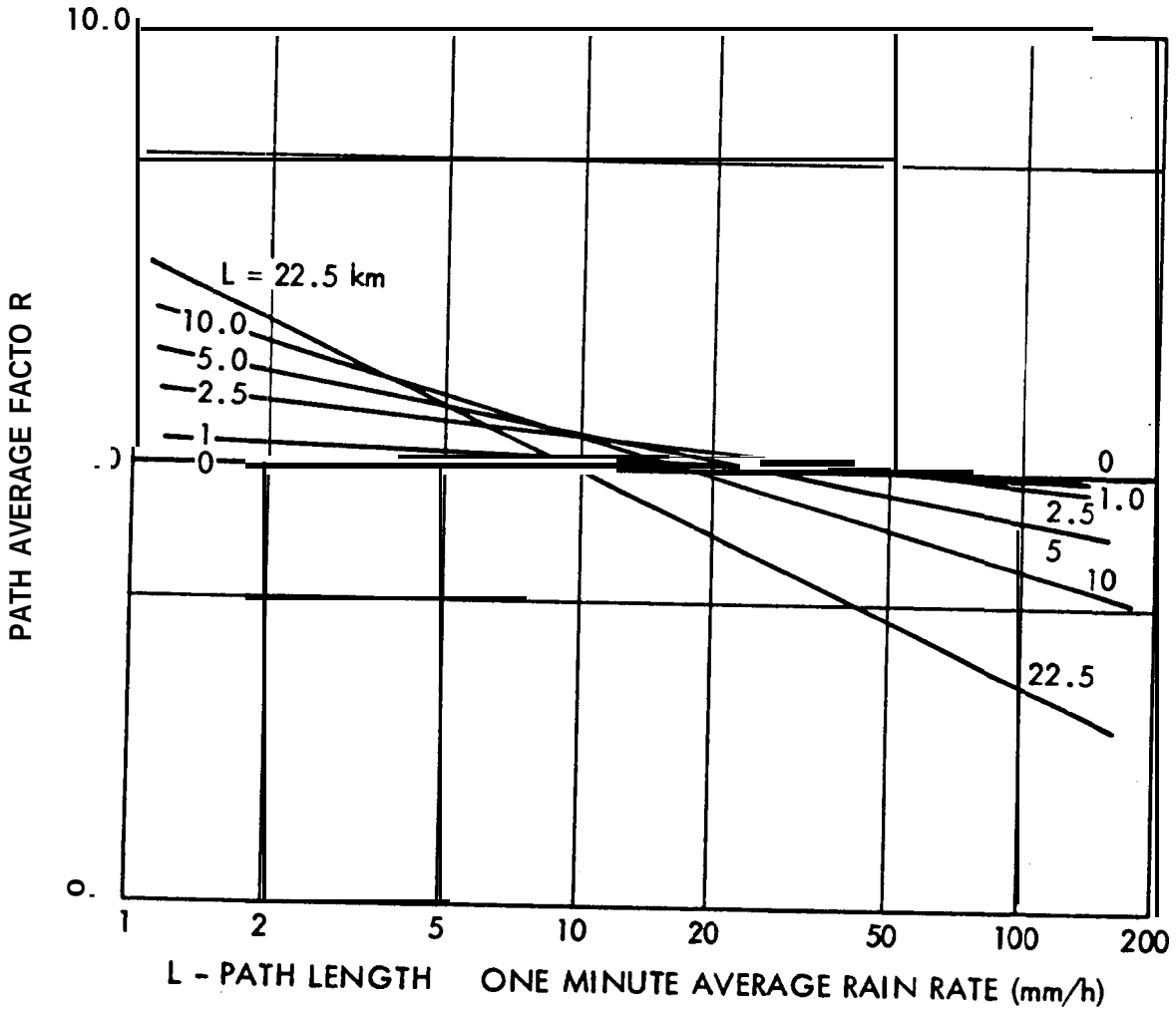

Figure 4.7. Effective path average factor for different path lengths and rates (CCIR, 1978).

Stutzman and Yen, 1986). The two-component model (Crane, 1982, 1985a) starts with an assumed value of attenuation and determines the separate probabilities that the attenuation can be caused by rain cells and surrounding rain debris.

4.3.3 Models of Attenuation Due to Rain

Several models of attenuation due to rain have been developed and refined and updated from time to time. The goal of the models is to provide statistically-based predictions of attenuation, and they encompass the three areas mentioned earlier - statistical data on rain rate, the calculation of the value of the attenuation constant from rain rate, and the spatial distribution of rain.

For locations of First Order Weather Stations in the United States and for locations having similar records elsewhere, data are available to provide statistical descriptions of rainfall. Lin (1977) and Lee (1979) describe and analyze procedures for obtaining the needed statistics from such data, which are published by the National Climatic Center in the United States. Earth stations, however, may well be located elsewhere than where weather stations are found, and for world-wide application it is desirable to divide the Earth into regions having similar rainfall characteristics and to attempt to obtain statistical descriptions of these characteristics. Selection of regions can be done on a large scale in rough accordance with the natural regions of- the Earth (Sec. 1.4). A number of variations of such classifications exist. They agree generaly on principal features but may disagree on detail and terminology. It has been suggested, however, that classifications made from biological, geographical, or agricultural viewpoints may need some modifications for telecommunications purposes (Segal, 1980). Figures 4.8 and 4.9 show the regions used in the Crane (1980) global model, and Fig. 4.10 shows regions of Canada, consistent generally with the CCIR 1982 model but modified somewhat by Segal (1986). The regions of the CCIR model are shown on a world-wide basis in Figs. 4.13 to 4.15

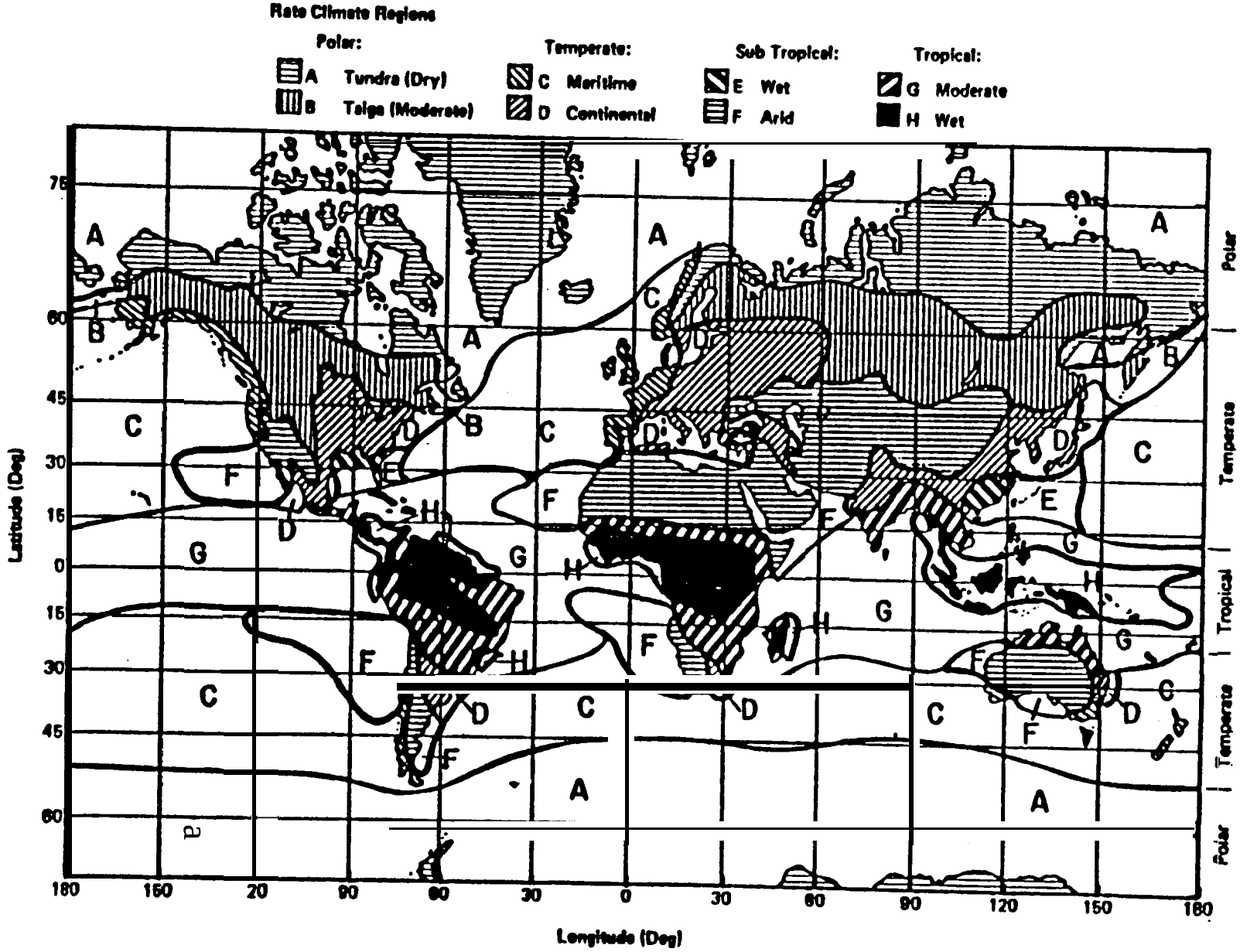

Figure 4.8. Global rain ra e regions (Crane, 1980).

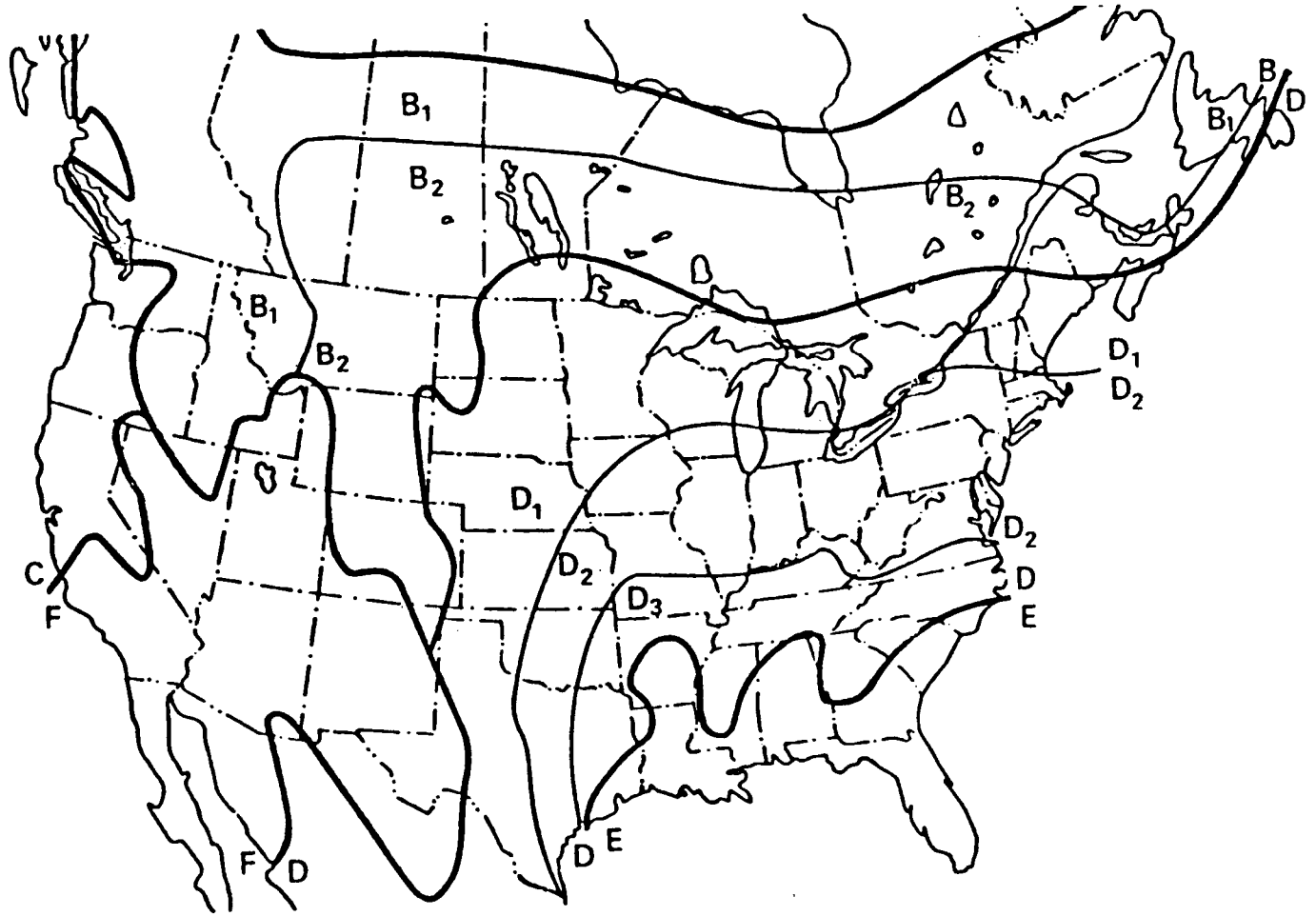

Figure 4.9. Rain rate regions of United States, as used in global model (Crane, 1980).

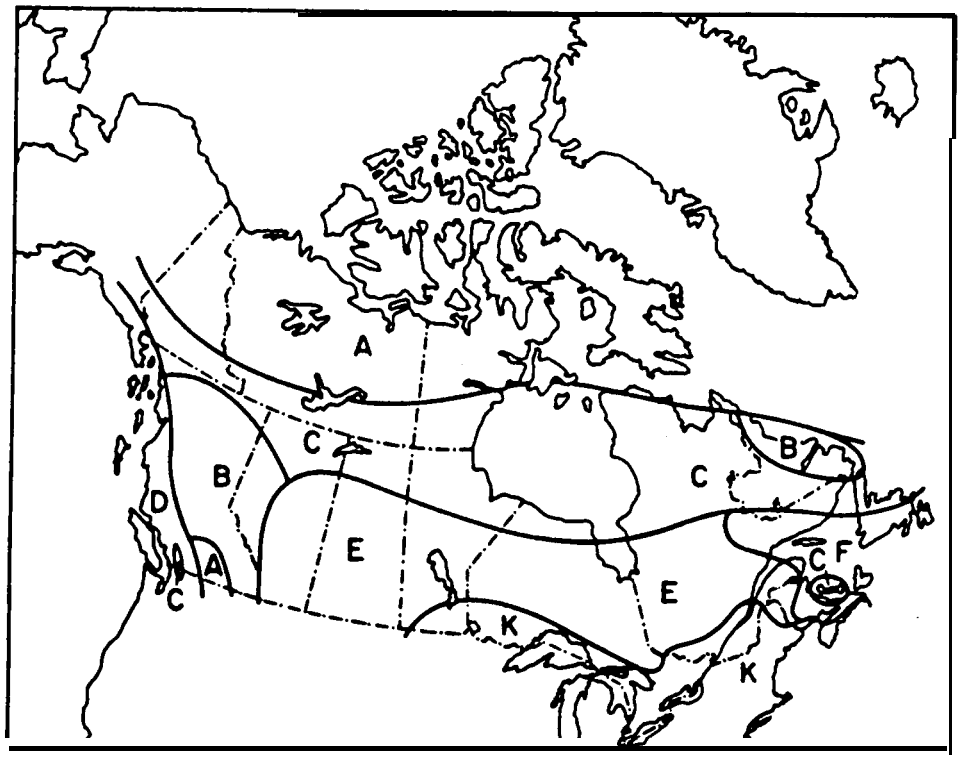

Figure 4.10. Rain rate regions of Canada, as defined by the CCIR and modified by Segal (1986).

The 1980 Global Model of Fig. 4.8 (No. 5 of this Sec. 4.3.3) involves 8 rain rate regions which correspond fairly well to the natural regions of the Earth (Trewartha, 1968; Sec. 1.4). As regions B and D for North America are subdivided, however, the Global Model can actually be considered to involve 11 regions. The modified 1982 CCIR Model (No, 8 of this Sec. 4.3.3) utilizes 14 rain rate regions, and these are based more closely on rain rate alone rather than natural regions. For example, whereas both models designate the arctic and antarctic regions as rain-rate region A, the Global Model restricts designation A to these regions while the CCIR model applies designation A to desert areas as well. Both high-latitude and desert areas have low rainfall, and that is the justification for designating both with the same symbol. The Global Model applies the designation F to deserts, Mediterranean areas, and to some temperate grassland and steppes whereas these three regions are actually quite different. The CCIR model applies the designation E to an even larger area including deserts, the Mediterranean area of southern California, and southern Canada, presumably because these areas may have roughly the same total rainfall. Southern California has hardly any thunderstorm activity, however, whereas the other areas have considerable thunderstorm activity. The type of rain as well as total amount is significant, and more detailed analyses and classifications for the occurrence of rain than those of the world-wide models can very well be utilized, especially for areas characterized by mountain ranges. The occurrence of rain can be very different in both total amount and type on opposite sides of mountain ranges.

Another case for which additional detail is desirable is that of the occurrence of rain as a function of time at given locations. The detail is desirable in order to obtain more reliable statistics about rain rates that are equaled or exceeded for small percentages of time. The averaging process can hide the occurrence of high rain rates for only a minute or a few minutes when rainfall is recorded for periods even as short as five minutes. It has become accepted that a one-minute raingauge integration time is a desirable compromise for recording rainfall. Much time and effort would be required to produce an adequate data base of one minute data, however, and attention has therefore been given to how to estimate one-minute rainfall data from longer-period data (CCIR, 1986c; Segal, 1986).

Characteristics of some of the models of rain attenuation will be described in this section. First we note that a good data base has been accumulated on attenuation due to rain on a number of paths. Analyses have been made of the comparative performance of several of the models to be described by use of this data base with differing conclusions (Crone, 1985a, 1985b; Stutzman and Yen, 1986). The interested reader or person dealing extensively with rain attenuation is advised to read the original papers, as it is not practical to provide detailed descriptions or comparisons showing the relative merits of the models or to provide numerical illustrations of all of them. Instead we include brief discussions of several of the models and use primarily the modified CCIR 1982 model to illustrate how the problem of rain attenuation can be treated. Numerical examples are given in Sec. 9.4. For the United States, however, we tend to favor using the rain-rate regions and values of the 1980 global model. Although the type of rain modeling described here is well developed, the opinion has been stated (Crane at Jan. 1986 meeting of NASA experimenters) that more effort is needed on other topics including fade duration and site diversity predictions.

1. Rice-Holmberg Model

Using a variety of meteorological data, Rice and Holmberg (1973) formulated a model which predicts distributions of t-minute point rainfall rites. The model gives the cumulative number of hours in a year that the rain rate may be expected to exceed a specified value durig t-minute periods, e.g. 5-minute periods, etc. The model involves the use of 3 basic parameters which are M, the annual rainfall in mm; β, the average annual ratio of thunderstorm rain to total rain ; and D, the average number of days for which the precipitation exceeds 0.25 mm. M and D are determined directly from recorded data, and β is derived from data on the greatest monthly values in mm and the average number of days with thunderstorms. In considering this model one can set $M = M_1 + M_2$ where M_1 represents thunderstorm or convective rain and M_2 stands for stratiform rain of relatively wide extent and long duration. Convective rain tends to involve high rain rates but only comparatively short periods. The parameter β represents the ratio Ml/M.

2. Dutton-Dougherty Model, Modified Rice-Holmberg Model

The Dutton-Dougherty model predicts total attenuation from precipitation, clouds, and clear air. For attenuation caused by rain it. uses a modified Rice-Holmberg model (Dutton, 1977). An incentive for modifying the Rice-Holmberg model is that while the original model provides P(R), the percent of time that rainfall rate R is exceeded, given values of R, it is difficult to invert to obtain R, given P(R). That is, if one wishes to determine the rain rate R that is exceeded 0.0 1 percent of the time, for example, it is difficult to do so by using the original Rice-Holmberg model. The modified Rice-Holmberg model overcomes this problem. Like the original model it uses the 3 parameters, M, β, and D. Stratiform rain is assumed to be uniform up to the rain cloud base and to decrease to zero at the storm top height, while convective rain is assumed to increase slightly, in terms of liquid water content, up to the rain cloud base and to then decrease to zero at the storm top height.

Some results of interest obtained by use of the Dutton-Dougherty model in computer form have been published for Europe (Dougherty and Dutton, 1978) and the United States (Dutton and Dougherty, 1979). The papers provide maps of Europe and the United States that show contours of one-minute rainfall rates in mm/h, corresponding to values equaled or exceeded for 1, 0.1, and 0.01 percent of the time. The papers also include contours of the standard deviation in mm/h of annual rainfall rates corresponding to the percentages mentioned above. Data for 30 years were used for the United States. In 1982, the Dutton-Doughert y model was improved to extend to rain rates exceeded for 'the low percentage of 0.001 (Dutton, Kobayashi, and Dougherty, 1982). The question of incorporating the concept of effective path length into the model was considered and re jetted, Instead a probability modification factor F is retained for modeling the variation of rain intensity in the horizontal direction. This factor multiplies the original percent of time p. that attenuation of a certain value is expected to obtain a lower value p. For determining the attenuation constant α, an expression like Eq. (4.11) is used except that in place Of rain rate R in mm/h the quantity L , liquid water content per unit volume, is employed.

3. Piecewise Uniform Rain Rate Model

The piecewise uniform model (Persinger et al., 1980) is a quasi-physical model developed to eliminate the need for effective path lengths. It involves the assumptions that the spatial rain rate distribution is uniform for low rates but becomes increasing y nonuniform as the peak rain rate increases. Total attenuation A is determined from

$$A = (L/N) \sum_{i=1}^{N} \alpha(R_i) \quad \text{“} \tag{4.17}$$

where L is the path length which is divided into N equal intervals, α is the attenuation constant corresponding to rain rate R_i of the ith division or cell. Two levels are used in the version reported here, with

$$R_l = R_1 \text{ for } 0 \le l \le CL, \quad R_l = R_x \text{ for } CL \le l < L \tag{4.18}$$

where

$$R_x = R_1 \text{ for } R_1 \le 10 \text{ mm/h}, \quad R_x = R_1(R_1/10)^x \text{ for } R_1 \ge 10 \text{ mm/h} \tag{4.19}$$

In terms of these quantities, the expression for A can be written as

$$A = [\, C\,\alpha(R_1) + (1 - C)\,\alpha(R_x)\,]\, L \text{ dB} \tag{4.20}$$

Based on experimental evidence for the eastern United States, C is taken to be 0.2 and x is taken to be -0.66. Path length L is found by using a height extent of rain H and a basal length B with H equal to 3.5 km for high latitudes above 40 deg, 4.0 km for mid latitudes, and 4.5 km for low latitudes below 33 deg. The quantity B is taken to be 10.S km. Then

$$L = H/\sin\theta \text{ for } \theta \ge \theta_0, \quad L = B/\cos\theta \text{ for } \theta \le \theta_0 \tag{4.21}$$

with $\theta_0 = \tan^{-1} H/B$ and θ the elevation angle.

4. Radar Modeling

The utility of radar for obtaining rainfall data was mentioned in Sec. 4.3.2, and the radar technique, with emphasis on bistatic scatter, is discussed in Sec. 4.5. Radar contributions to rain-attenuation modeling were described by Goldhirsh and Katz (1979). Data on the intensity of rainfall along a path or over an area and also as a function of height can be obtained.

An extensive amount of radar data have been obtained at Wallops Island, VA by use of the SPANDAR S-band radar, much of it at time - that COMSTAR beacon measurements at 28.56 GHz were also being made (Goldhirsh, 1982a). Radar reflectivity Z can be related to rain rate R by

$$R = u\ Z^{v} \qquad \text{mm/h} \qquad (4.22)$$

where u and v are drop-size dependent. A disdrometer, an instrument for measuring drop-size distributions} has been developed and utilized in studies reported here. Values of u and v used for Laws and Parsons and Marshall and Palmer distributions can be derived from Eqs. (4.56) and (4.57). Goldhirsh has shown that the radar data he obtained agreed well with attenuation values measured by use of the COMSTAR beacon. Also he has shown that the radar data can be extrapolated to other locations with good agreement with directly measured data. The radar technique is readily adaptable to space diversity studies, and this application is the subject of a 1982 paper (Goldhirsh, 1982b). The ability to employ radar data for the modeling of both single and joint probability cumulative fade distributions at various path elevation angles and frequencies received attention in a 1984 paper (Goldhirsh, 1984).

5. 1980 Global Model

This model, described by Crane (1980) divides the world into the eight rain-rate regions shown in Fig. 4.8. The United States is covered by five regions, with two, B and D, subdivided as shown in Fig. 4.9. Figure 4.11 or Table 4.4, giving rain rates exceeded for various percentages of time, provide the needed rain rate data. For determining values of attenuation constant α_p use is made of $\alpha_p = aR^b$ where R is rain rate. For Canada, however, we recommend using the regions of Fig. 4.10, supplied by Segal (1986). Rates

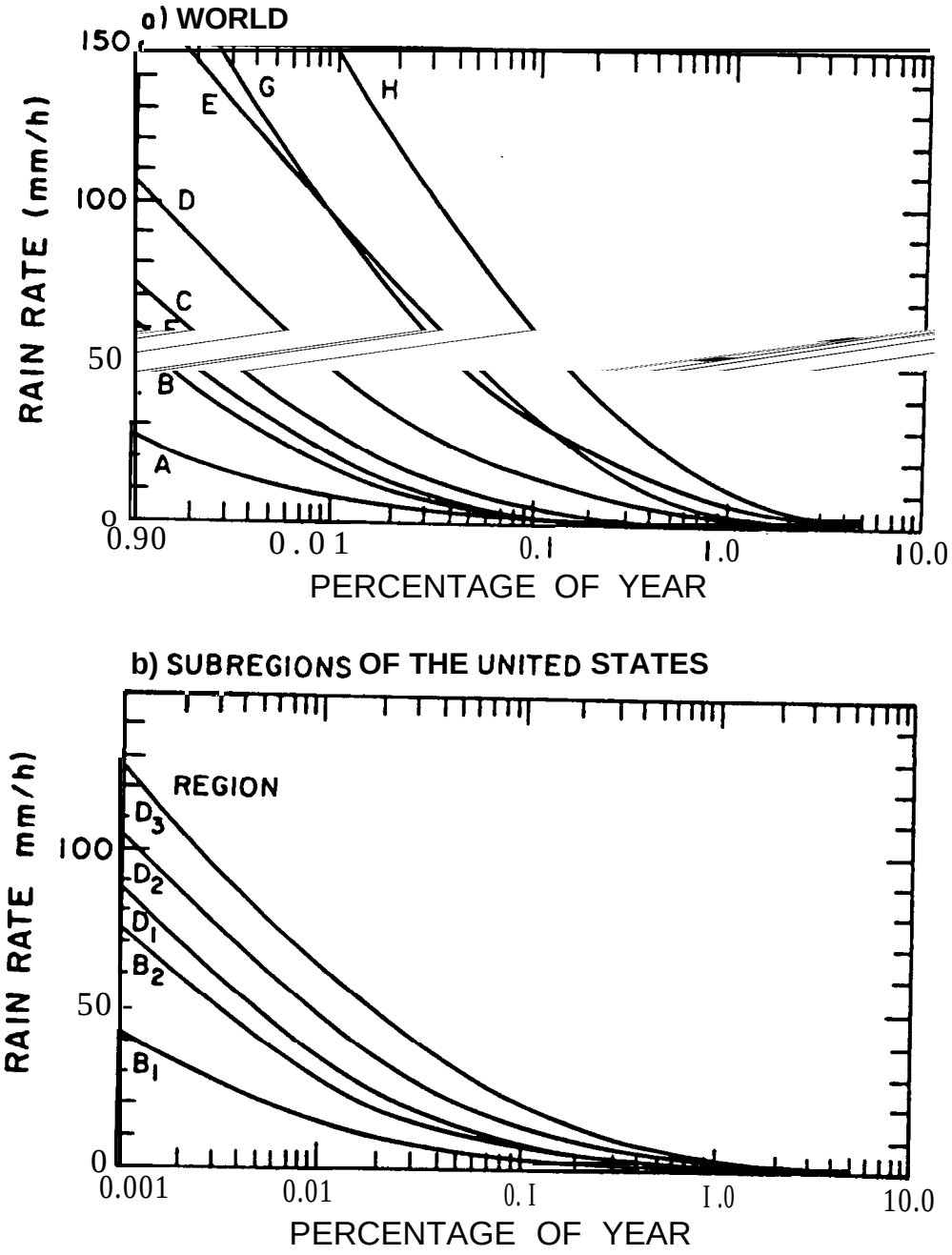

Figure 4.11. Rain rates as a function of percent of year exceeded, for 1980 Global Model.

exceeded as a function of percentage of time for the Canadian regions are shown in Table 4.5. Believing the relation mentioned in Sec. 4.3.2 for the spatial distribution of rainfall to be inadequate because of the nonlinear relation between rain rate and attenuation constant, Crane used numerical differentiation to obtain relative path rain-rate profiles showing that when high point rain rates occur, the most intense rain is found close to the sampling location. When rain rates are low at the sampling location, however, higher rain rates are likely at distances in excess of 6 km away. Approximation of the profiles by exponential functions leads to an expression for attenuation along a horizontal path of length D that involves three such functions as follows.

$$A(R, D) = \alpha R^{\beta} \left[\frac{e^{\mu\beta d} - 1}{\mu\beta} b^{\beta} e^{c\beta d} + \frac{b^{\beta} e^{c\beta D}}{c\beta} \right] \quad (4.23)$$

$$d < D < 22.5 \text{ km}$$

$$A(R,D) = \alpha R^{\beta} \left[\frac{e^{\mu\beta D} - 1}{\mu\beta} \right] \qquad 0 < D < d \qquad (4.24)$$

with A in dB, R in mm/h, and αR^{β} the expression of Eq. (4.11) but with α and β used in place of a and b.

$$\mu = \frac{\ln (bed)}{d} \quad (\text{d in km}) \qquad b = 2{,}3\ R^{-0.17}$$

$$c = 0.026\text{-}0.03 \ln R \qquad d = 3.8 - 0.6 \ln R$$

For elevation angles θ greater than 10 deg, D is given by

$$D = (Ho - H_g) / \tan \theta \qquad [4.25]$$

where H_0 is the height of the O deg isotherm from the Method II curves of Fig. 4.7 and H_g is the height of the surface. Attenuation As along a path of length L is given by

$$A_S = [\ L\ A(R,\ D)\ ]/D = [\ A(R,\ D)\ ]/\cos\theta \qquad (4.26)$$

for $\theta \geq 10$ deg. For $\theta \leq 10$ deg, see Appendix 4.1. The original

Table 4.4 Rain Rates Exceeded as a Function of Percentage of Year, for Regions A to H of 1980 Global Model.

Percentage of Year	Rain Rates Exceeded (mm/h)											
	A	B		C		D=D_2	D_3	E	F	G	H	
		'1	'2	'1								
0.001	29	45	58	70	78.	90	108	126	165	66	185	253
0.002	21	34	44	54	62	72	89	106	144	51	157	220.5
0.005	13.5	22	28.5	35	41	50	64.5	80.5	118	34	120.5	178
0.01	10.0	15.5	19.5	23.5	28	35.5	49	63	98	23	94	147
0.02	7.0	11.0	13.5	16	18	24	35	48	78	15	72	119
0.05	4.0	6.4	8.0	9.5	11	14.5	22	32	52	8.3	47	86.5
0.1	2.5	4.2	5.2	6.1	7.2	9.8	14.5	22	35	5.2	32	64
0.2	1.5	2.8	3.4	4.0	4.8	6.4	9.5	14.5	21	3.1	21.8	43.5
0.5	0.7	1.5	1.9	2.3	2.7	3.6	5.2	7.8	10.6	1.4	12.2	22.5
1.0	0.4	1.0	1.3	1.5	1.8	2.2	3.0	4.7	6.0	0,7	8.0	12.0

A percentage of 0.01 of a year corresponds to 53 minutes.

global model used a path reduction factor mentioned in See, 4.3.2 and calculated by a procedure like that of the 1 982 CCIR model [Eq. (4.33)].

6. Two-Component Model

When using models such as the 1980 Global Model and the 1982 CCIR Model, one first determines the rain rate R that is expected to be exceeded for p percent of the time. The attenuation constant α_p corresponding to R is then calculated. The two-component model, however, starts with values of attenuation and determines the separate probabilities of exceeding this attenuation because of convective rain cells on the one hand and widespread rain debris on the other. The mme of the model is derived from its recognition and separate treatment of the two types of rain, intense rain in localized cells of the order of a couple of kilometers in diameter and rain of lesser intensity but greater areal extent. Recall that the Rice-Holmberg and Dutton-Dougherty models separated rainfall in a somewhat similar way into thunderstorm or convective rain of generally short duration and stratiform rain of generally wide extent and longer duration.

The two-component model was introduced in 1982 (Crane, 1982). A step-by-step description is igen as an appendix in the original paper. A similar treatment of a revised version is given as an appendix in Crane (1985a). Certain features of the model are described in Appendix 4.2 of this handbook.

7. SAM (Simple Attenuation Model)

The simple attenuation model employs the procedure of the 1982 CCIR rain model (No. 8, following) to predict rain rate as a function of percentage of time and calculates the attenuation constant from rain rate by use of the usual empirical relation, Eq. (4.11). The improved version of SAM described in 1986 (Stutzman and Yen, 1986) uses the 1982 CCIR values of a and b for horizontal and vertical polarization, which values also allow determination of a and b for arbitrary polarization [Eqs. (4. 12) and (4. 13)]. The original SAM model used the a and b values of Olsen, Rogers, and Hedge (1978). A distinctive feature of SAM is its treatment of the spitial distribution of rainfall. Considering that the treatment of this same topic is unnecessarily complicated in the 1 980 Global Model, the authors use a simpler assumption about

the variation of rainfall with distance from the ground station location. For a rain rate R. at the station equal to or less than 10 mm/h, the rain rate is assumed to be constant along the path so that

$$R(1) = R. \text{ for } R. \leq 10 \text{ mm/h}$$

For a rain rate equal or greater than 10 mm/h, R (ℓ) is assumed to be given by

$$R(\ell) = R_o e^{[-\gamma \ln (R_o/10) \ell \cos \theta]}, \quad R_o \geq 10 \text{ mm/h} \qquad (4.27)$$

This expression applies for $\ell \leq L$ where $L = (H - Ho)/\sin \theta$. The expressions for $R(\ell)$ are substituted into

$$A(R_o) = \int_o^L a R(\ell)^b d\ell$$

leading to the results that

$$A(R_o) = a R.^b L \qquad R. \leq 10 \text{ mm/h} \qquad (4.28)$$

$$A(R_o) = a R_o^b \frac{1 - e^{[-b\gamma \ln (R_o/10) L \cos \theta]}}{b\gamma \ln (R_o/10) \cos \theta}, \quad R_o \geq 10 \text{ mm/h} \qquad (4.29)$$

A value of 1/14 is used for y in the 1986 version of SAM.

The 1982 CCIR model uses an effective path length equal to $L r_p$, where r_p is a path reduction factor, and its procedure is actually simpler than SAM in this respect. The CCIR approach is empirical and has been designated as provisionaL

8. Modified 1982 CCIR Model

The rain rate regions of the 1982 CCIR model are shown in Figs. 4.13 - 4.15, and the rain-rate values for these regions are given in Table 4.5. In addition, contours of the rain rate exceeded for 0.01 percent of the time are provided in Figs. 9.8-9.10. The attenuation constant α corresponding to these rain-rate values is found by using aR^b_p with values of a and b from Table 4.3. The latest revisions of CCIR Reports 563 and 564 give the expression of Eq. (4.30) for determining the height extent H of rain

(CCIR, 1986c,d) For latitudes # less than 36 deg, the height extent of rain H is taken as 4.0 km, and for $\phi \geq 36$ deg one uses

$$H = 4.0 - 0.075\ (\ \phi - 36^\circ\ )\ \text{km} \qquad \phi \geq 36^\circ \qquad (4,30)$$

In the first edition of this handbook the dotted modification of the Method 1 curve of Fig. 4.6 was recommended, and persons concerned with attenuation from rain at lower latitudes should be alert to the possibility that lower heights than 4.0 km mY still be applicable. In either case whether using Eq. (4.30) or ig. 4.6, the height H to be used is the height equaled or exceeded with a probability of 0.01. The length L though rain is determined by

$$L = H/\sin\theta \ \text{km} \qquad (4.31)$$

for elevation angles θ greater than 10 deg. For angles less than 10 deg use

$$L = \frac{2H}{[\ \sin^2\theta + 2\ (H/a)\ ]^{1/2} + \sin\theta} \ \text{km} \qquad (4.32)$$

where a is effective earth radius.

Attenuation A in dB is determined for theperecentage of 0.01 from

$$A = a_P\, L\, r_P \qquad (4.33)$$

where α_p and L are discussed above and r_p is an empirical path reduction factor factor given by

$$`P = \frac{1}{1 + 0.045\ D} \qquad (4.34)$$

where D = L cos θ is the horizontal projection of L. Previously the form 90/ (90 + 4D) was used; the numerical values of these two expressions are essentially identical. To determine attenuation A_p equaled or exceeded with a probability other than 0.01, the latest recommendation is to use

$$A_p = A_{0.01}\, 0.12\, p^{-(0.546 + 0.043 \log p)} \qquad (4.35)$$

Previously the procedure (CCIR, 1983b) was to use

$$A_p = c\, A_{0.01}\, p^{-d}$$

Values were supplied for the constants c and d and Fig. 4.12 was also given. Although replaced by the CCIR by Eq. (4.35), we retain Fig. 4.12 in this chapter for reference purposes. The original 1982 CCIR model distinguished maritime and continental climates, using what in 1983 became known as Method 1 for maritime climates and Method 2 for continental climates (CCIR, 1983b). Note that Method 1 (original or modified dotted form) provided the height equalled or exceeded with a probability of 0.01 percent. Method 2, however, provided heights for probabilities of 0.001, 0.01, 0.1, and 1 percent. Both Methods 1 and 2 have been replaced with Eq. (4.30) now used for the height of rain H in both cases. The latest procedure nevertheless follows the general plan of Method 1 in that a height is determined only for a probability of 0.01. Then attenuations for other percentages are determined by use of Eq. (4.35),

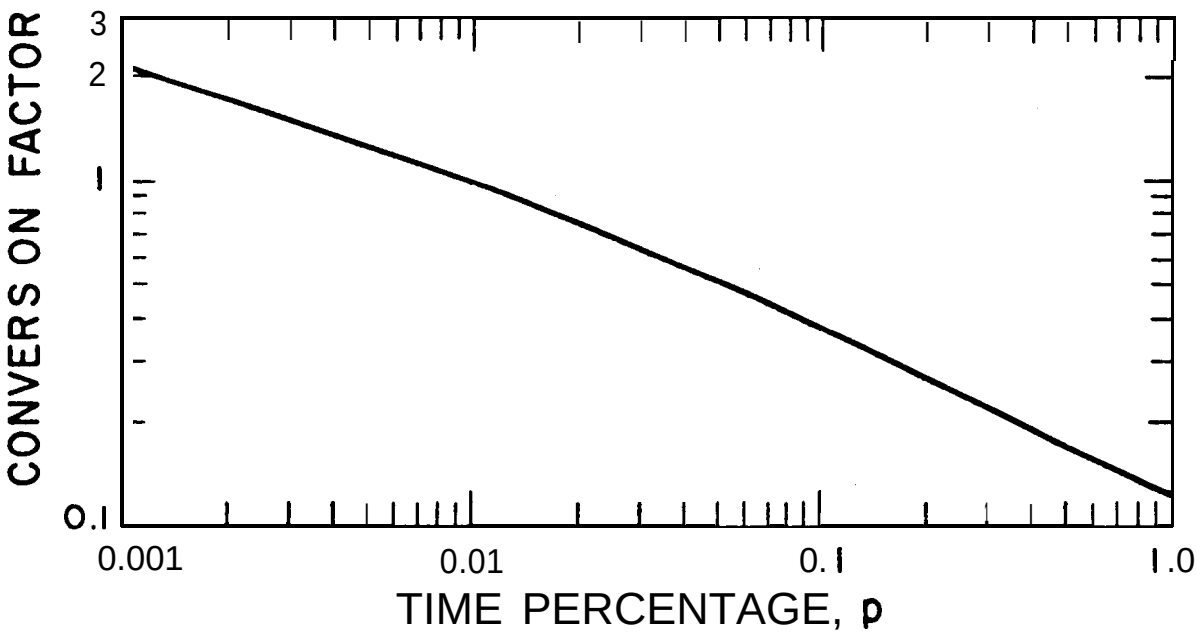

Figure 4.12. Factor cp^{-d} for conversion of the rain attenuation exceeded for 0.01 perecent of the time $A_{0.01}$ to that exceeded for p percent of the time, as given in CCIR (1983b). The latest recommended procedure, however, is to use Eq. (4.35).

Table 4.5 Rain Rates Exceeded as a Function of Percentage of Year, for Regions A to P of 1982 CCIR Model.

Percentage of Year	Rain Rates Exceeded (mm/h)													
	A	B	C	D	E	F	G	H	J	K	L	M	N	P
1.0		1	-	3	1	2				2		4	5	12
0.3	1	2	3	5	3	4	7	4	13	6	7	11	15	34
0.1	2	3	5	8	6	8	12	10	20	12	15	22	35	65
0.03	5	6	9	13	12	15	20	18	28	23	33	40	65	105
0.01	8	12	15	19	22	28	30	32	35	42	60	63	95	145
0.003	14	21	26	29	41	54	45	55	45	70	105	95	140	200
0.001	22	32	42	42	70	78	65	83	55	100	150	120	180	250

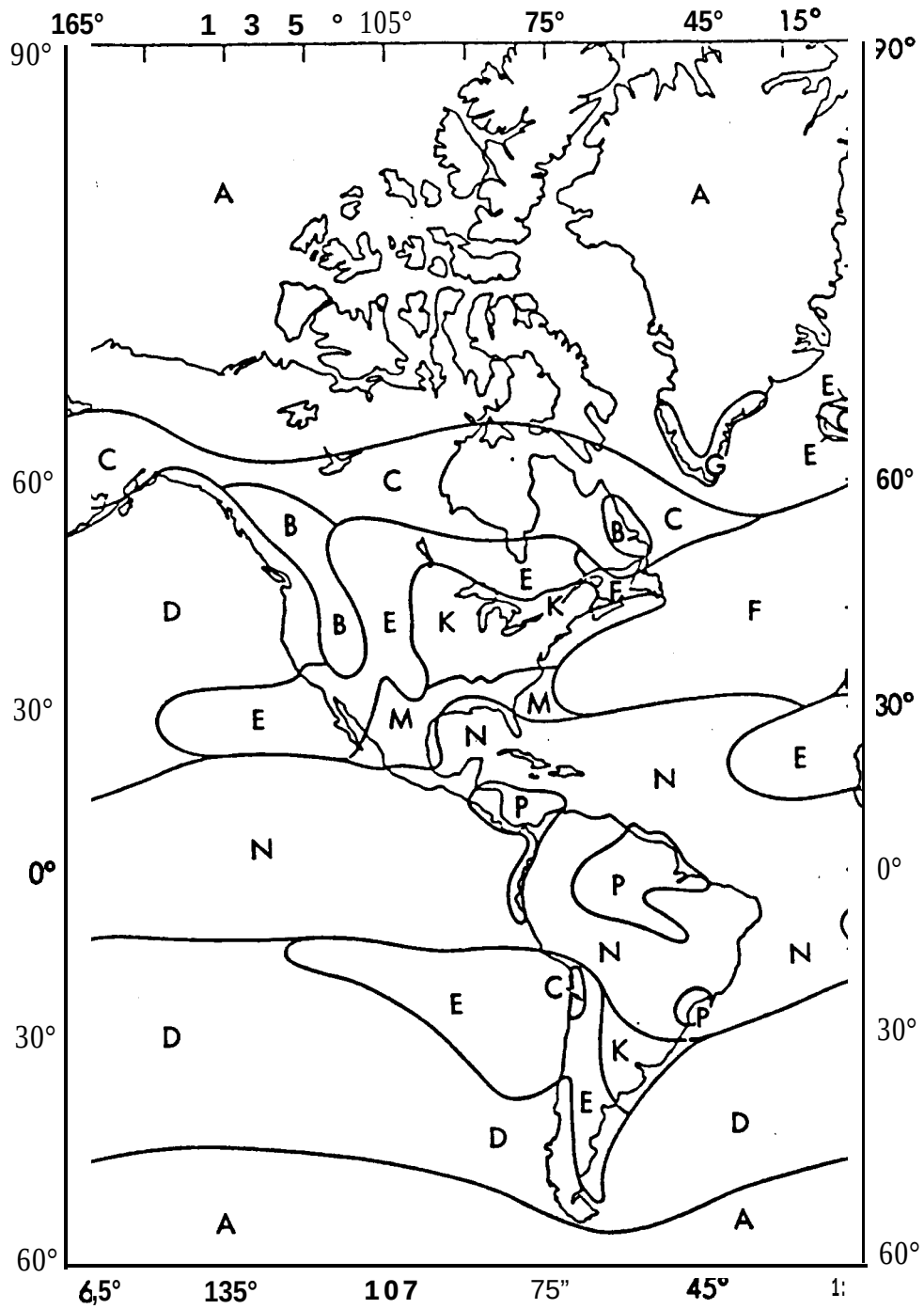

Figure 4.13. Rain-rate regions of the Americas (CCIR, 1986c).

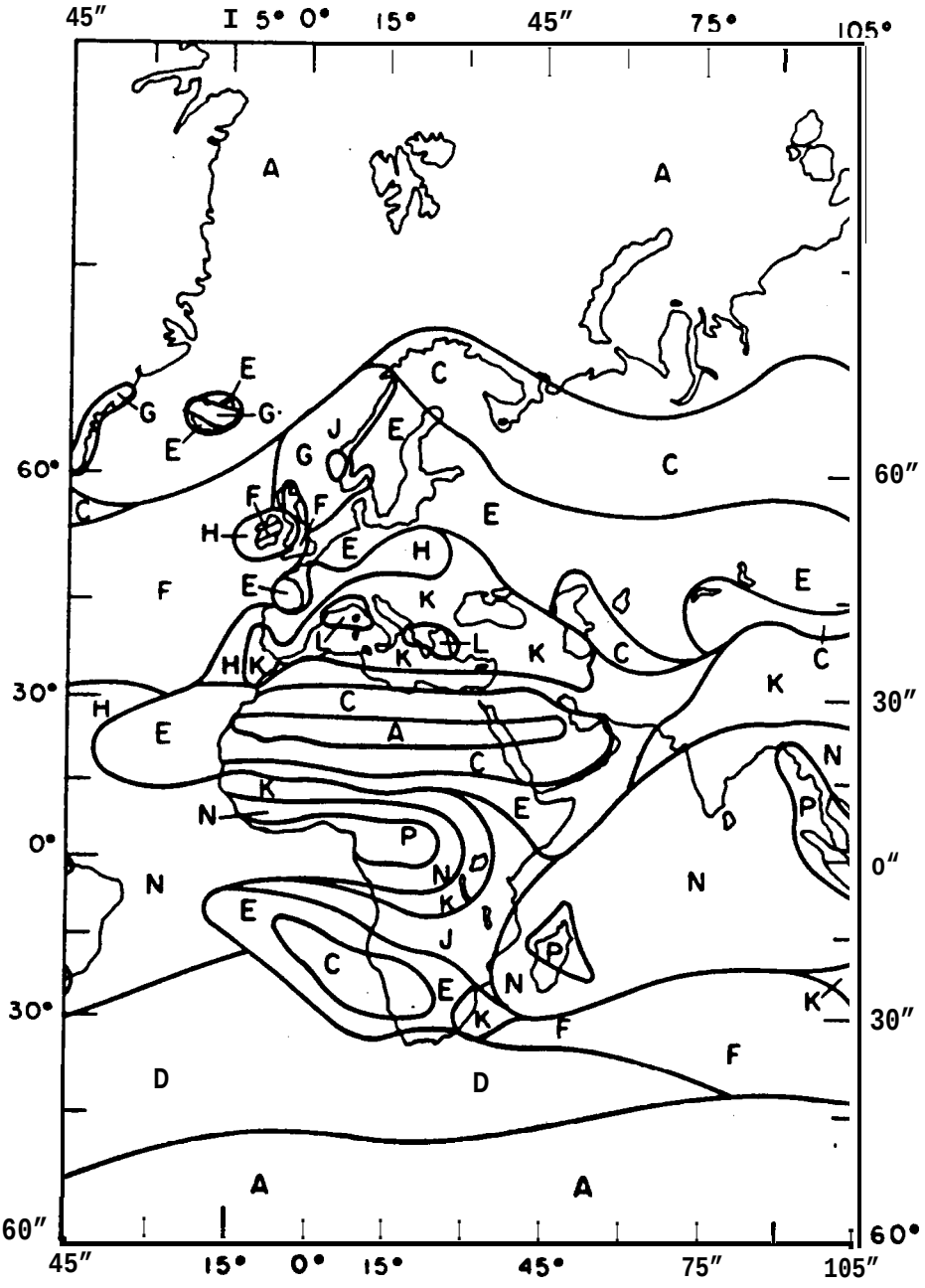

Figure 4.14. Rain-rate regions of Europe and Africa (CCIR, 1986c).

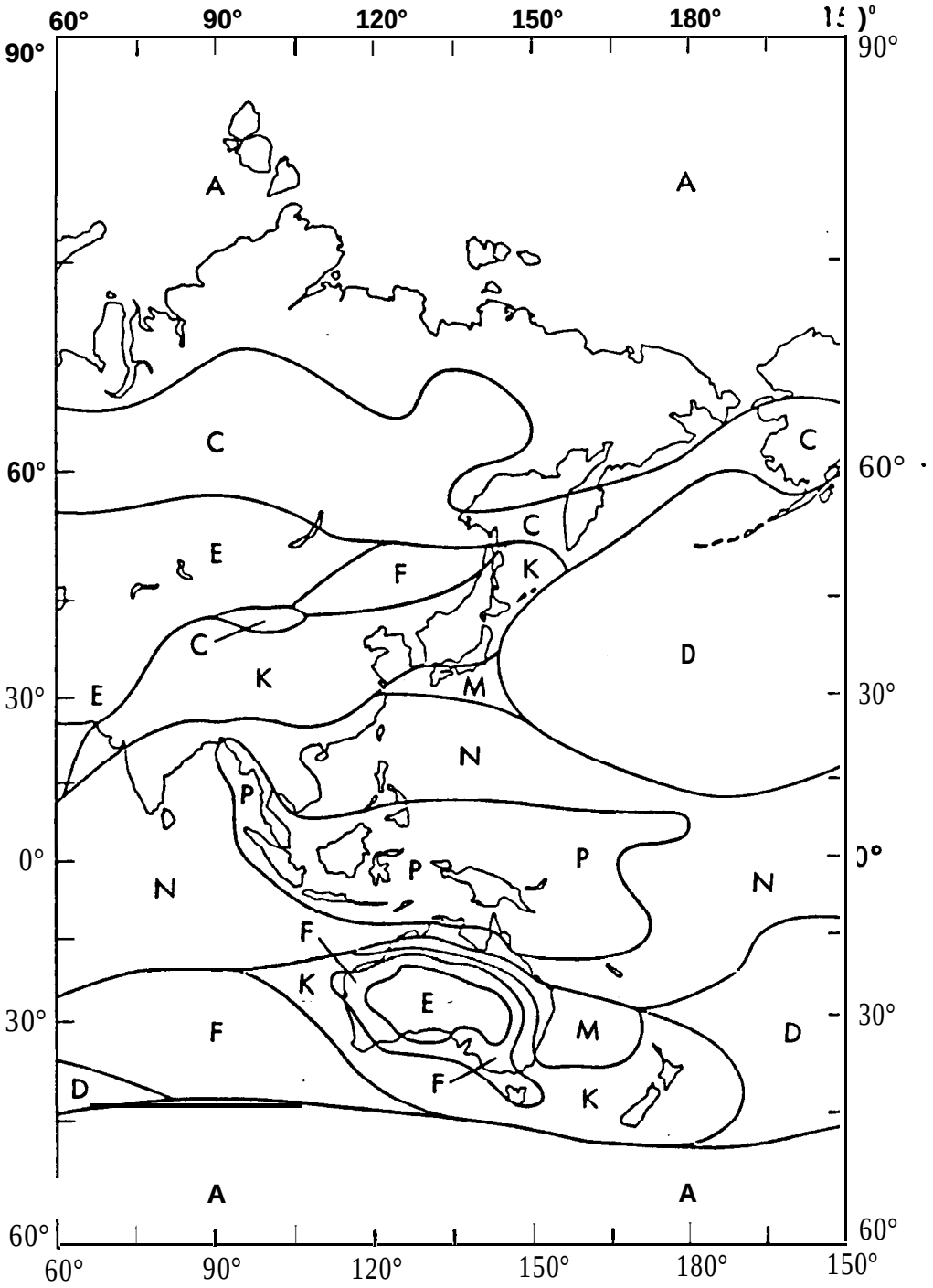

Figure 4. 15. Rain-rate regions of Asia and Oceania (CCIR, 1986c).

4.4 DEPOLARIZATION DUE TO PRECIPITATION

The term depolarization refers to a degradation or change in polarization, as from purely vertical linear polarization to linear polarization at an angle slightly different from vertical, This latter condition is equivalent to a combination of vertical and horizontal polarization. Such an effect can be caused by precipitation.

It is highly desirable in many circumstances to be able to use two orthogonal polarizations on the same path, but the ability to do so may be limited to some degree by antenna characteristics or depolarization caused by precipitation or some other phenomena. The two linear polarizations are generally referred to as vertical and horizontal, but for earth-space paths the polarizations tend to be rotated somewhat from the local vertical and horizontal axes (Dougherty, 1980). The two orthogonal circular polarizations are right and left circular polarization (Sec. 2.1, 1). Two orthogonal polarizations are sometimes referred to as cross polarizations, and a wave of the opposite or orthogonal polarization that is produced by a process of depolarization is known as a cress-polarized wave. The production of a cross-polarized wave may result in unacceptable interference between orthogonally polarized channels of the same path.

In considering transmission through rain, theratio of the power of the wanted or copolarized wave to the power of the unwanted or crosspolarized wave is pertinent. Letting E_{11} and E_{22} represent electric field intensities of copolarized waves and E_{12} and E_{21} represent field intensities of crosspolarized or unwanted waves and expressing the ratio in dB, it may have the form of 20 log E_{11}/E_{12}, for example. The first subscript represents either a reference or original polarization, and the second subscript represents an actual (resulting or final) polarization. Thus E_{12} is a field intensity having polarization 2. It may have been derived from a wave of original polarization 1, or polarization 1 may merely be the reference polarization of the system. This kind of ratio is referred to by the term cross polarization discrimination (XPD). For the example mentioned above

$$XPD = 20 \log (E_{11}/E_{12}) \qquad (4.36)$$

The use of the term discrimination is pertinent in some cases, but the notation XPD has been used also to describe the polarization of a wave whether a process of discrimination is involved or not, For example, if a receiving system has a linear horizontally polarized antema but an incident wave is linearly Polarized at an angle τ from the horizontal, it may be said that

$$XPD = 20 \log \cot r \tag{4.37}$$

as $E_{1j} = E. \cos \tau$ and $E_{12} E_0 \sin \tau$, where E_0 is a reference intensity and El_1 and E_{12} are components along horizontal and vertical axes.

Rather than using XPD to describe the state of polarization, use can be made of its reciprocal, depolarization D, which has the form of

$$D = 20 \log (E_{12}/E_{11}) \tag{4.38}$$

A high XPD value of 40 dB, for example, corresponds to a small depolarization of -40 dB; a low XPD value of 10 dB corresponds to a large depolarization of - 1 O dB.

Depolarization due to precipitation is caused by the nonspherical shape of rain drops and ice crystals; spherical drops do not cause depolarization. Depolarization would not occur in the case of spheroidal drops either if the field intensity vector of a linearly polarized wave were to lie strictly parallel to either the long or short axes of the drops.. In the general case, however, - the roughly spheroidal drops tend to be canted or tilted with respect to the electric field intensity vectors. Wind contributes to canting and, even in the case of apparently vertical fall, the drops normally exhibit a distribution of canting angles. Differential attenuation and phase shift of field components parallel to the long and short axes of drops cause depolarization. The effect of differential attenuation is shown in a qualitative way in Fig. 4.16. A circularly polarized wave is equivalent to the combination of two linearly polarized waves that differ by 90 deg in both spatial configuration and electrical phase, and depolarization occurs for circularly polarized waves also. Indeed, it develops that depolarization tends to be worse for circularly polarized waves than for linearly polarized waves.

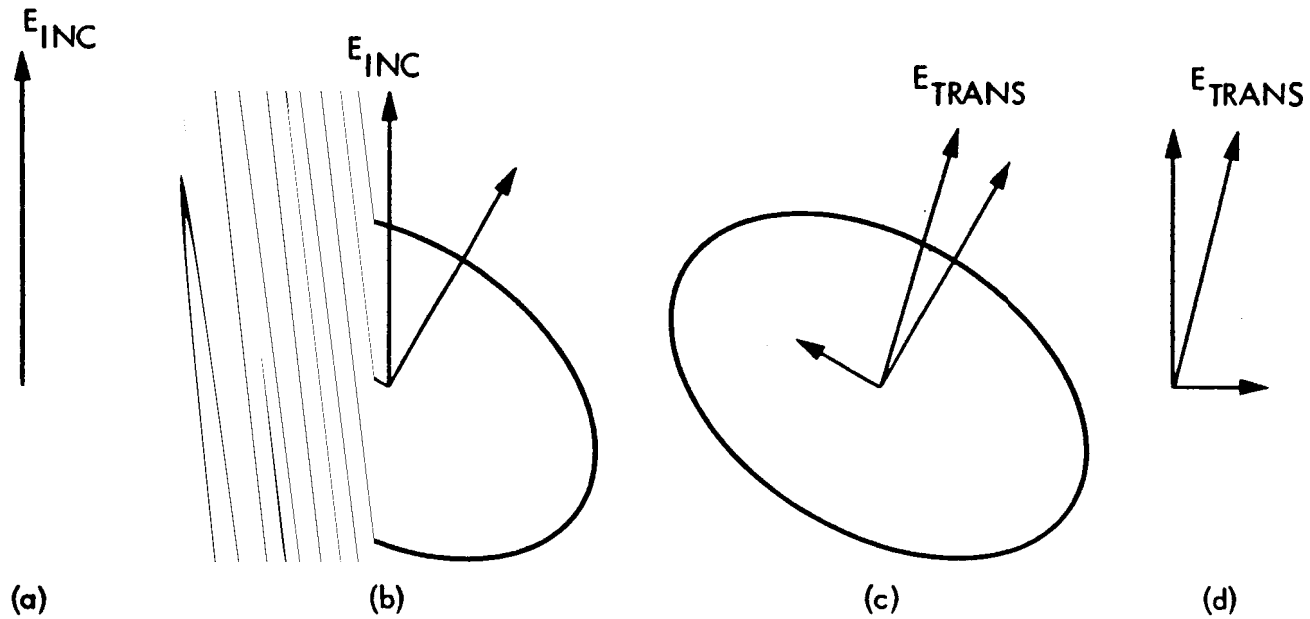

Figure 4.16. An incident vertically polarized wave emerges from rain no longer strictly vertical after experiencing differential attenuation of components parallel to the major and minor axes of raindrops.

Analysis of depolarization D in terms of differential attenuation and phase shift has been presented by Chu (1980). A form for D for circular polarization is

$$D_{cir}\,(dB) = 10 \log \{ 1/4 [\sqrt{(Aa)^2 + (\Delta\beta)^2 L }]^2 e^{-4\sigma^2}) \quad (4.39)$$

where Aa is the differential attenuation constant and $\Delta\beta$ is the differential phase constant. The quantity L is the length of the path through rain. A factor of 2 dB is sometimes added to take account of the possible contribution to depolarization of ice particles occurring above the level of the O deg C isotherm. When the logarithm of the exponential factor is taken, the result, designated as κ squared, " has the form

$$\kappa^2 = 17.37\ \sigma^2 \quad (4.40)$$

with σ in radians or

$$\kappa^2 = 0.0053\ \sigma^2 \quad (4.41)$$

with σ in degrees, where σ is the standard deviation of the raindrop canting angle ϕ, measured from the horizontal, along a path at a particular instant of time. This quantity κ^2 can be set equal to zero as a conservative design procedure (CCIR, 1986d). For linear polarization

$$D_{lin}(dB) = D_{cir}(dB) + 10 \log[1/2\ (1 - \cos 4\tau\ e^{-8\sigma^2_m})] \pm \Delta A'/2 \quad (4.42)$$

In this expression τ is the tilt angle from the horizontal of the electric field intensity vector of the linearly polarized wave. The quantity σ_m is the standard deviation in radians of the mean raindrop canting angle ϕ_m from path to path and storm to storm. For σ_m in deg, $8\sigma^2_m$ can be replaced by $\kappa^2_m = 0.0024\ \sigma^2_m$, with 5 deg a suitable value for σ_m. CCIR Report 722-2 (1986d) points out that κ^2 and κ^2_m depend on factors other than the canting angle distribution and should not be thought of as related to canting angle only. The quantity AA' is given by

$$\Delta A' = 5 \log (|\overline{a_{vv}}|^2/|\overline{a_{hh}}|^2) \quad (4.43)$$

where a_{vv} and a_{hh} are attenuation constants for vertical and horizontal polarization. The sign of $\Delta A'/2$ is chosen to give the lowest value of D for quasivertical polarization. In Eq. (4.42), the logarithm of a quantity less than unity is indicated, and this logarithm is therefore negative. The equation thus shows that the depolarization is generally less for linear polarization than for circular polarization. For τ = 45 deg, however, depolarization is essentially the same for linear and circular polarization. The value of τ can be taken as 45 deg for circular polarization, and it is for tilt angles away from 45 deg that linear polarization has an advantage over circular polarization. The distribution of canting angles ϕ is over a range around the horizontal. The angle shown in Fig. 4.16 is exaggerated in order to make the effect of differential attenuation obvious. In Chu's 1980 paper he gives examples of the application of the above relations to extrapolation from measured values of D on one path to values to be expected on other paths.

An alternative form of the right side of Eq. (4.39) for is

$$D_{cir}(dB) = 20 \log \left[1/2 \sqrt{(\Delta\alpha_o)^2 + (\Delta\beta_o)^2}\ L \cos^2\theta\ e^{-20^2} \right] \quad (4.44)$$

which is based upon

$$\sqrt{(\Delta\alpha)^2 + (\Delta\beta)^2} = \sqrt{(A_o a)^2 + (\Delta\beta_0)^2 \cos^2\theta}$$

where Aa_o and $\Delta\beta_o$ refer to an elevation angle θ. This equation shows that depolarization decreases with increasing elevation angle.

Values of $\sqrt{(A a_o)^2 + (\Delta\beta_o)^2}$ are given in Fig. 4.17 as a function of rain rate and frequency. That depolarization should decrease with increasing elevation angle can be understood by considering the outline of raindrops as seen from the direction of incident waves at θ = O deg and at θ = 90 deg. Differential attenuation and phase are maximum for an elevation angle of O deg

for which the shape seen looking an incident k vector, representing the direction of propagation of an incident wave, is elliptical. At the other extreme for which cos θ = O, however, the shape seen when looking along an incident k vector at an elevation angle of 90 deg is circular. This symmetrical shape is not conducive to depolarization. Equations (4,42)-(4.44) together with Fig. 4.17 show the dependence of depolarization on rain rate, frequency, polarization, tilt angle, elevation angle, and path length L, which can be determined with the help of Fig. 4.6.

In a later paper (Chu, 1982), the basis is shown for expressing depolarization D and crosspolarization XPD in terms of total attenuation A in dB for frequencies above 10 GHz, as is the case for the common empirical expression for XPD. For this purpose note that $\sqrt{(\Delta\alpha_o)^2 + (\Delta\beta_o)^2}$ is proportional to frequency (Fig. 4.17)$_0$ Also it develops that total attenuation A in dB is proportional to frequency" squared in the 10 to. 30 GHz range. Thus $\sqrt{(\Delta\alpha_o)^2 + (\Delta\beta_o)^2}\, L\ f/A$ is a constant. Introducing this constant into Eq. (4.44)

$$D_{cir}(dB) = 20 \log \left[\sqrt{(\Delta\alpha_o)^2 + (\Delta\beta_o)^2}\, L\ f/A\ \right] - 17.3702$$

$$-6.02-20 \log f + 40 \log \cos\theta + 20 \log A \qquad (4.45)$$

The term -20 log f appears to correct for the addition of 20 log f into Eq. (4.44) where it did not originally appear, and 20 log A is introduced for the same reason. Keep inmindthat AisindB. The quantities $\Delta\alpha_0$ and $\Delta\beta_o$ refer to an elevation angle of 0 deg, and 40 log cos θ accounts for the $\cos^2\theta$ factor of Eq. (4.44). To convert to XPD one can merely change the signs of the terms. Doing this but taking the first three terms as equal to a constant $(XPD)_o$, one obtains

$$(XPD)_{cir}(dB) = (XPD)_o + 20 \log f_{GHz} - 40 \log \cos\theta - 20 \log A_{dB} \qquad (4.46)$$

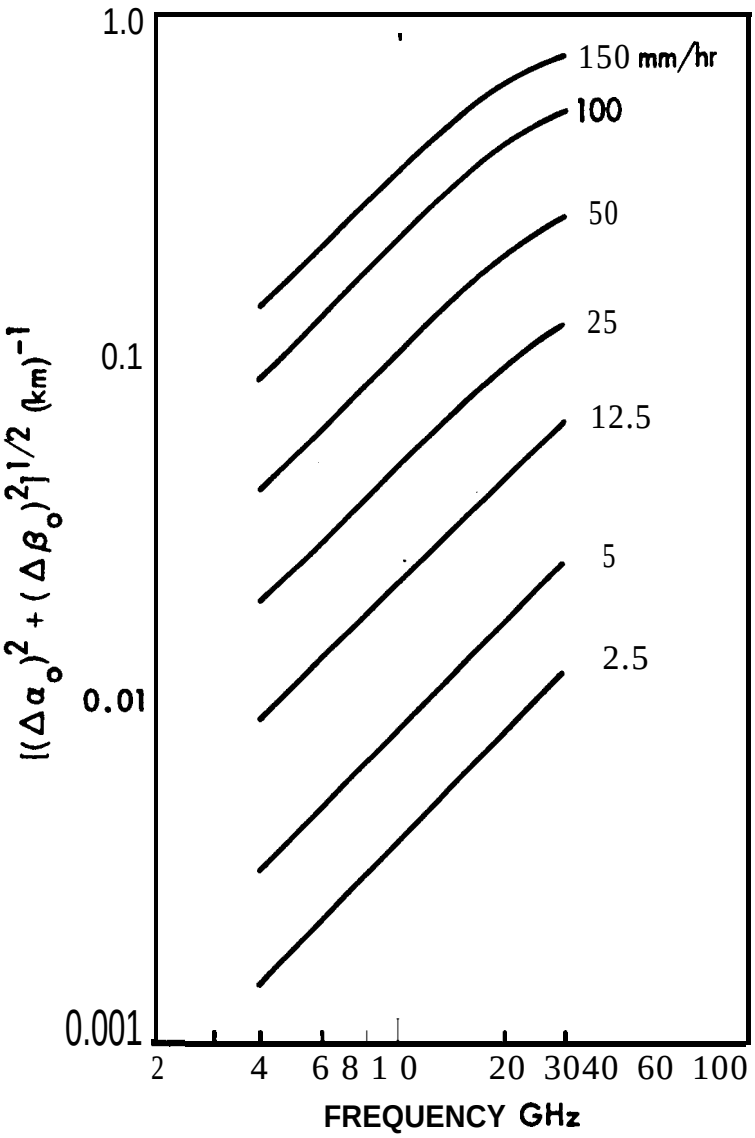

Figure 4.17. Differential propagation constant at zero elevation angle as a function of frequency and rain rate (Chu, 1980).

and

$$(XPD)_{lin}(dB) = (XPD)_{cir} - 10 \log 1/2 [\, i - \cos 4\tau\, e^{-\kappa^2 m} \,] \,. \pm \Delta A'/2 \quad (4.47)$$

Chu has determined by analysis of experimental data that these relations give satisfactory results with $(XPD)_o$ set equal to i 1.5. Thus his form of the equation is

$$(XPD)_{cir}(dB) = 11.5 + 20 \log f_{GHz} - 40 \log \cos \theta - 20 \log A_{dB} \quad (4.48)$$

The quantity AA' of Eq. (4.47) can be converted to the form

$$\Delta A' = O.15 A_{dB} \cos^2\theta \cos 2\tau \quad (4.49)$$

Equation (4.48) is similar to the expression given in CCIR Report 722-2 (CCIR, 1986d), namely

$$XPD\,(dB) = 30 \log fGH_z - 40 \log \text{Cos e} - 10 \log [1/2(1 - \cos 4\tau \cdot e^{-\kappa^2 m})] - 20 \log A_{dB} \quad (4.50)$$

This relation applies to both linear and circular polarization, with τ = 45 deg for circular polarization. Note that the same type of variation with elevation angle and polarization tilt angle is shown in Eqs. (4.47) and (4.48) on the one hand and Eq. (4.50) in the other case. The principal difference in the two treatments is that Eq. (4.48) has $11.5 + 20 \log f_{GHz}$ where Eq. (4.50) has $30 \log fGH_z$. Chu (1982) asserts that better agreement is obtained between theorv and experiment when $11.5 + 20 \log f_{GHz}$ is used in place of $30 \log f_{GHz}$.

An important point about Eqs. (4.47), (4.48), and (4.50) is that they include a term $-20 \log A_{dB}$, whereas Eqs. (4.39), (4. 42), and (4.44) are in terms of differential attenuation and pbase. Being able to express XPD in terms of A is a useful step but is only a suitable approach for frequencies above about 8 GHz.

As this handbook refers to frequencies below 10 GHz, it is appropriate to emphasize the application of Eqs. (4.42-4.44) for our purposes. Furthermore these relations have the virtue of being closer to basic physical concepts.

A principal reason why Eq. (4.50) is not suitable for frequencies below about 8 GHz is that differential phase shift tends to play an important role below 8 GHz. Attenuation, and therefore differential attenuation as well, decreases rapidly below 10 GHz, but differential phase shift does not decrease so rapidly. This condition can be understood by reference to Figs. 4.3a and 4. 3b. Figure 4.3b shows that the imaginary part, m_i, of the complex index of refraction of a medium containing raindrops, decreases rapidly below 10 GHz. However Fig. 4.3a shows that the real part, m_r, stays nearly constant over a range below 10 GHz.

Occurrences of low values of XPD (or high depolarization) when attenuation is low have been attributed to ice crystals, which cause small attenuation but can degrade XPD. Relations between XPD and attenuation that are developed for rain should not be extended to low values of attenuation for this reason (Bostian and Allnut, 1979). Data on rain depolarization at 4 GHz have been obtained by Yamada et al. (1977). For such relatively low frequencies attenuation values are low and are not useful for predicting XPD either as previously mentioned. A treatment of XPD that differs from that of Eq. (4.50) with respect to dependence on tilt angle τ and canting angle σ and also includes a numerical treatment of the effects of ice crystals is given in CCIR, 1986b. Note that a relation between between κ of Eq. (4.50) and σ is shown following Eq. (4.42).

4.5 BISTATIC SCATTER FROM RAIN

In considering the propagation of signals through a region of rainfall, interest commonly enters on the degree of attenuation of signals propagating in the forward direction. Another effect is that rain scatters energy into all directions, with a resulting potential for interference with earth-space or terrestrial line-of-sight telecommunication systems. Such scatter is referred to as bistatic scatter, using the term bistatic as in radar operations when transmitter and receiver are at different locations.

The process of bistatic scatter can be described as follows. The power density P in W/m^2 at a distance R_1 from a transmitter having a power output of W_T watts and an antenna gain of G_T is given by

$$P = \frac{W_T G_T}{4\pi (R_1)^2} \tag{4.51}$$

At the location where the power density is P, consider a target having a radar cross section of ηV m^2 where η is the cross section per unit volume and V is the total volume taking part in the scattering process. In the present case V is the common volume of the transmitting and receiving antennas as shown in Fig. 4.18.

Considering the common scattering volume to be small so that the distance from the transmitter to any part of it is R_1 and the distance from the receiver to any part of the volume is R_2, the common volume is presumed to radiate isotropically the power incident upon it so that the received power W_R, intercepted by an antenna with an effective area of AR at the distance of R_2, is given by

$$W_R = \frac{W_T G_T \eta V A_R}{(4\pi)^2 (R_1)^2 (R_2)^2} \tag{4.52}$$

Making use of the relation between gain G and effective area A, namely $G = 4\pi A/\lambda^2$, the equation can be put into the form

$$\frac{W_R}{W_T} = \frac{G_T G_R \eta V \lambda^2}{(4\pi)^3 (R_1)^2 (R_2)^2 L} \tag{4.53}$$

where a loss factor L has been added to take account of attenuation of the incident and scattered waves and any polarization mismatch. Assuming for simplicity that Rayleigh scattering takes place, the cross section per unit volume η is given by

$$\eta = \frac{\pi^5}{\lambda^4} \left| \frac{K_c - 1}{K_c + 2} \right|^2 \sum d^6 \qquad m^2/m^3 \qquad (4.54)$$

where Kc is the complex index of refraction of water at the frequency in question and summation is shown over all of the drop diameters d within a unit volume. This summation is commonly represented by the symbol Z so that

$$\eta = \frac{\pi^5}{\lambda^4} \left| \frac{K_c - 1}{K_c + 2} \right|^2 Z \qquad m^2/m^3 \qquad (4.55)$$

Empirical relations have been derived between Z and rain rate R. For the Laws and Parsons distribution

$$z = 400\ R^{1.4} \qquad (4.56)$$

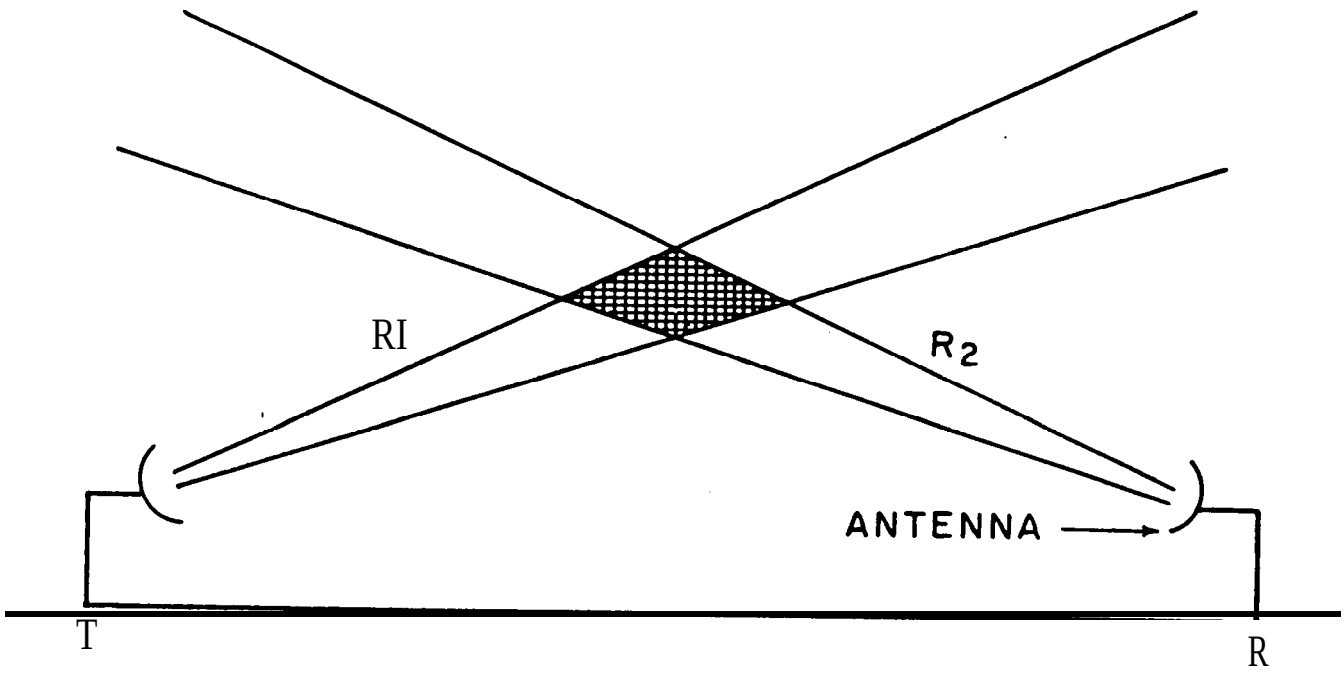

Figure 4.18. The cross-hatched area is a two-dimensional representation of the common volume of the transmitting and receiving antennas.

with Z in mm^6/m^3. Another form of the relation betwen Z and R, which is a slight revision of the relation proposed by Marshall and Palmer and is based on their drop-size distribution is

$$z = 200\ R^{1.6} \tag{4.57}$$

In monostatic radar observations of rainfall η can be determined from Eq. (4.53) and Z can then be determined from Eq. (4.55) except that for monostatic radar R_1 and R_2 are the same and V is proportional to distance squared so that W_R/W_T varies inversely with distance squared if rain fills the common scattering volume. In Eqs. (4.54) and (4.55), all lengths are in meters. To convert from Z in m^6/m^3 to mm^6/m^3 for use in Eqs. (4.56) and (4.57) multiply by 1018.

For calculation of interfering signal levels one can assume rain rates R and calculate A and η for insertion into Eq. (4.53).

4.6 CONCLUSION

Much of the interest in effects of precipitation on telecommunications has been directed to frequencies above 10 GHz, but the various models of attenuation due to rain are generally applicable below 10 GHz as well. Attenuation and noise due to precipitation may be important for frequencies as low as 8 GHz or lower and may need to be taken into account for frequencies as low as 4 GHz. Depolarization, the production of cross polarized components that have polarizations orthogonal to the original polarizations, increases with attenuation above about 8 GHz. For lower frequencies, differential phase shift rather than differential attenuation tends to make the major contribution to depolarization, and sigrificant depolarization may take place for frequencies as low as 4 GHz. Backscatter from precipitation is important in radar observations at frequencies as low as those of the L band (e.g. 1500 MHz), and bistatic scatter from rain is a potential source of interference for telecommunication system operations at frequencies this low as well as at higher frequencies.

Water in the form of a thin layer or film over a radome or reflector and as the tiny drops of clouds or fog, as well as in the form of the larger drops of rain, can affect the performance of telecommunications systems. It has been pointed out that a given water content integrated along a path causes more attenuation when the water is in the form of a thin slab than when it occurs as fog or rain. Hogg and Chu (1975) used the water content of a slab 1 mm in thickness, corresponding to a rain of 25 mm/h over a one-km path or fog of 0.1 g/m^3 over a 10-km path, to illustrate this point. Avoiding the use of radomes and using blowers to eliminate water films are means for minimizing system degradation due to water films.

Effects of clouds are considered in the following Chap. 5. Among the effects are a slight range delay, above that due to the gaseous constituents of the atmosphere. The same effect occurs for rain, for which the excess range or time delay can be determined from the real part of the complex index of refraction m_c of Sec. 4.1 by taking $\int \mathrm{Re}\,(m_c - 1)\,dl = \int (m_r - 1)\,dl$, namely the integral of the real part of m_c minus one over the path. Further consideration of range delay due to liquid water, whether of the tiny drops of fog or the larger drops of rain, can be found in Sec. 5.1.

The companion NASA Reference Publication 1082 (03), which applies to frequencies from 1 O to 100 GHz, povides extensive coverage of propagation effects caused by rain (Ippolito, Kaul, and Wallace, 1983).

REFERENCES

Arnold, H. W. , D. C. Cox, and A. J. Rustako, "Rain attenuation at 10-30 GHz along earth-space paths: elevation angle, frequency, seasonal, and diurnal effects," IEEE Trans. Commun., vol. COM-29, pp. 716-721, No. 5, 1981.

Bostian, C. W. and J. E. Allnut, "Ice crystal depolarization on satellite-earth microwave radio paths," Proc. IEEE, vol. 126, p. 951, 1979.

Bostian, C. W., T. Pratt, and W. L. Stutzman, "Results of a three-year 11.6 GHz, low-angle experiment using the SIRIO satellite." IEEE Trans. Antennas Propagat., vol. AP-34, pp. 58-65, Jan. 1986.

CCIR, "Rain attenuation prediction," Dec. P/ 10S-E, Geneva: Int. Telecomm. Union, 1978.

CCIR, "Attenuation and scattering by precipitation and other atmospheric particles," Report 721-2 in Vol. V, Propagation in Non-ionized Media, Recommendation and Reports of the CCIR, 1986. Geneva: Int. Telecomm. Union, 1986a.

CCIR, "Propagation data required for space telecommunication systems," Report 564-3 in Vol. V, Propagation in Non-ionized Media, Recommendation and Reports of the CCIR, 1986. Geneva: Int. Telecomm. Union, 1986b.

CCIR, "Radio meteorological data," Report 563-3 in Vol. V, Propagation in Non-ionized Media, Recommendations and Reports of the CCIR, 1986. Geneva: Int. Telecomm. Union, 1986c.

CCIR, "Cross-polarization due to the atmosphere," Report 722-2 in Vol. V, Propagation in Non-ionized Media, Recommendation and Reports of the CCIR, 1986. Geneva: Int. Telecomm. Union, 1986d.

CCIR, "Data bank for earth-space propagation," Dec. 5/19-E, Geneva: Int. Telecomm. Union, 1983a.

CCIR, "Propagation data required for space telecommunication systems," Proposed modification to Report 564-2, Dec. 5/10-E. Geneva: Int. Telecomm. Union, 1983b.

Chu, T. S., "Microwave depolarization of an earth-space path," Bell System Tech, Jour., vol. 59, pp. 987-1007, July-Aug., 1980.

Chu. T. S., "A semi-empirical formula for microwave depolarization on earth-space paths," IEEE Trans. Commun, vol. COM-30, pp. 2550-2554, 1982.

Crane, R. K., "Prediction of attenuation by rain," IEEE Trans. Commun., vol. COM-28, pp. 1717-1733, Sept. 1980.

Crane, R. K., "A two-component rain model for the prediction of attenuation statistics," Radio Sci., vol. 17, pp. '1371-1387, Nov.-Dee. 1982.

Crane, R. K., "Comparative evaluation of several rain attenuation prediction models," Radio Sci., vol. 20, pp. 843-863, JulyAug. 1985a.

Crane, R. K., "Evaluation of global and CCIR models for estimation of rain rate statistics," Radio Sci., vol. 20, pp. 865-879, July-Aug. 1985b.

Dougherty, H. T. and E. J. Dutton, "Estimating year-to-year varabilit y of rainfall for microwave applications," IEEE Trans. Commun., vol. COM-26, pp. 1321-1324, Aug. 1978.

Dutton. E. J., Earth-space Attenuation Prediction Procedures at 4 to 16 GHz, OT Report 77-123, May 1977.

Dutton, E. J. and H. T. Dougherty, "Year-to-year variability of rainfall for microwave applications in the U.S.A.," IEEE Trans. Commun., vol.COM-27, pp. 829-832, May 1979.

Dutton, E. J., H. K. Kobayashi, and H. T. Dougherty, "An improved model for earth-space microwave attenuation distribution prediction," Radio $ci., vol. 17, pp. 1360-1370, Nov.-Dee. 1982.

Flock, W. L., Electromagnetics and the Environment: Remote Sensing and Telecommunications. Englewood Cliffs, NJ: PrenticeHall. 1979.

Goldhirsh, J. and I. Katz, "Useful experimental results for earth-satellite rain attenuation modeling," IEEE Trans. Antennas Propagat., vol. AP-27, p. 413-415, May 1979.

Goldhirsh, J., "Slant path rain attenuation and rain rate statistics associated with the COMSTAR beacon at 28.56 GHz for Wallops Island, Virginia over a three-year period," IEEE Trans. Antennas Propagat., vol. AP-30, pp. 191-198, March 1982a.

Goldhirsh, J., "Space diversity performance prediction for earth-satellite paths using radar modeling techniques," Radio Sci., vol. 17, pp. 1400 -1410, Nov.-Dee. 1982b.

Goldhirsh, J., "Slant path rain attenuation and path diversity statistics obtained through radar modeling of rain structure," IEEE Trans. Antennas Propagat., vol. AP-32, pp. 54-60, Jan. 1984.

Hogg, D. C. and T. S. Chu, "The role of rain in satellite communications," Proc. IEEE, vol. 63, pp. 1308-1331, Sept. 1975.

Ippolito, L. J., 11.7 GHz Attenuation and Rain Rate Measurements with the Communications Technology Satellite (CTS), NASA Tech. Memo. 80283. Greenbelt, MD: NASA, 1978.

Ippolito, L. J., R. D. Kaul, and R. G. Wallace, Propagation Effects Handbook for Satellite Systems Design, NASA Reference Pub. ~ . ~ a -DC: NASA Commun. Div., June 1983.

Kaul, R., D. Rogers, and J. Bremer, A Compendium of Millimeter Wave Propagation Studies Performed by NASA, ORI Tech. Report, NASA Contract NAS5-24252, 1977.

Kerker, M., The Scattering of Light and Other Electromagnetic Radiation. New York: Academic Press, 1969.

Kerr, D. E. (ed.), Propagation of Short Radio Waves. Vol. 13, Rad. Lab. Series. New York: McGraw-Hill, 1951.

Laws, J. O. and D. A. Parsons, "The- relation of drop size to intensity," Trans. of AGU, pp. 452-460, 1943.

Lee, W. C. Y., "An approximate method for obtaining rain rate statistics for use in signal attenuation estimating," IEEE Trans. Antennas Propagat., vol. AP-27, pp. 407-413, May 1979.

Lin, S. H., "Nationwide long-term rain rate statistics and empirical calculation of i 1 -GHz microwave rain attenuation," Bell System Tech. J., vol. 56, pp. 1581-1604, Nov. 1977.

Marshall, J. S. and W. M. Palmer, "The distribution of raindrops with size," J. Meteorology, vol. 5, pp. 165-166, Aug. 1948.

Nackoney, O. G. and D. Davidson, "Results of 11.7-GHz CTS rain distribution measurements at Waltham, MA," Radio Sci., vol. 17, pp. 1435-1442, Nov.-Dee. 1982.

Olsen, R. L., D. V. Rogers, and D. B. Hedge, "The aR^b relation in the calculation of rain attenuation," IEEE Trans. Antemas Propagat., vol. AP-26, pp. 318-329, March 1978.

Persinger, R. R., W. L. Stutzman, R. E. Castle, and C. W. Bostian, "Millimeter wave attenuation rediction using a piecewise uniform rain rate model," IEEE Trans. Antennas Propagat., vol. AP-28, pp. 149-153, March 1980.

Pruppacher, H. R. and R. L. Pitter, "A semi-empirical determination of the shape of cloud and rain drops," J. Atmos. Sci., vol. 28, pp. 86-94, Jan. 1971.

Rice, P. L. and N. R. Holmberg, "Cumulative time statistics of surface-point rainfall rates, " IEEE Trans. Commun., vol. COM-21, pp. 1131-1136, Oct. 1973.

Ryde, J. W., "The attenuation and radar echoes produced at centimetre wavelengths by various meteorological phenomena," in Meteorological Factors in Radio-Wave Propagation, pp. 169-189. London: The Physical Society, 1946.

Segal, B., "A new procedure for the determination and classification of rainfall rate climatic zones, " URSI Commission F Open Symposium, Lennoxville, Quebec, 26-30 May 1980.

Segal, B., "The influence of raingauge integration time on measured rainfall-intensity distribution functions," to be published in Journal of Atmospheric and Oceanic Tech. vol. 3, Dec. 1986,

Stutzman, W. L. and K. M. Yen, "A simple rain attenuation mode for earth-space radio links operating at 10-35 GHz," Radio Sci. vol. 21, pp. 65-72, Jan. -Feb. 1986.

van de Hulst, H. C., Light Scattering by Small Particles. New York: Wiley, 1957.

Vogel, W. J., "Measurements of satellite beacon attenuation at 11.7, 19.04, and 28.56 GHz and radiometric site diversity at 13.6 GHz," Radio Sci., vol.17, pp. 1511-1520, Nov.- Dec. 1982.

Yamada, M., A. Ogawa, O. Furuta, and H. Yuki, "Rain depolarization measurement by using INTELSAT-IV satellite in 4-GHz band at low elevation angle," URSI Commission F Symposium Pmt., pp.409-419, LaBaule, France, 1977.

Zuffery, C. H., A Study of Rain Effects on Electromagnetic Waves in the 1-600 GHz Range," M. S. thesis. Boulder, CO: Department of Electrical Engineering, U. of Colorado, 1 972 (reprinted in 1979).

APPENDIX 4.1

1980 GLOBAL MODEL

For elevation angles θ less than or equal to 10 deg in the 1980 Global Model, it is stated that D, the horizontal extent of rain, is given by

$$D = E\psi \tag{A 4.1}$$

with

$$\psi = \sin^{-1}\left\{\frac{\cos\theta}{H_o + E}\left[(H_g + E)^2 \sin^2\theta + 2E(H_o - H_g) + H_o^2 + H_g^2\right]^{1/2} - (H_g + E)\sin\theta\right\} \tag{A 4.2}$$

The quantity E is the effective earth radius and the value of 8500 km, corresponding to k = 4/3 (Sec. 3.2, Table 3.2) is suggested. H_o is the height of the 0 deg C isotherm, and H_g is the height of the station.

Also for $\theta \leq 10$ deg, the path length L is given by

$$L = \left[(E + H_g)^2 + (E + H_o)^2 - 2(E + H_g)(E + H_o)\cos\psi\right]^{1/2} \tag{A 4.3}$$

APPENDIX 4.2
TWO-COMPONENT MODEL

The vertical extent of each of the two types of rain considered in the two-component model is taken to be a function of latitude, For convective rain cells, the height H_c is given by

$$H_C = 3.1 - 1.7 \sin [\, 2 (\theta' - 45^o) \,] \quad k \quad m \qquad (A4.4)$$

where θ' is latitude. For rain debris the height H_d is given by

$$‘_d = 2.8 - 1.9 \sin [\, 2 (\theta' - 45^o) \,] \quad k \quad m \qquad (A4.5)$$

The horizontal projections of these heights, D_c and D_d respectively, are found for elevation angles greater than 10 deg from

$$D_c = (H_c - Ho)/ \tan \theta \qquad (A4.6)$$

$$‘_d = (f\text{-}l_d - Ho)/ \tan\theta \qquad (A4.7)$$

where θ is elevation angle and $H_{\_}$ is station height. More complicated expressions are given for angles less than 10 deg. The horizontal extent WC of rain cells, taken to be 2.2 km originally, is modeled in the revised version in accordance with

$$W_c = 1.87 R^{-0.04} \quad km \qquad (A4.8)$$

and for debris the horizontal variation of rain rate is modeled by

$$‘_d = 29.7 R^{-0.34} \quad km \qquad (A4.9)$$

The procedure for the two-component model involves determining D_c and D_d as indicated above. Values of attenuation A in dB are used to obtain initial estimates of R, namely R_i, for rain cells, and R_i is used in Eq. (A4.8) to obtain a value for W_c. Likewise an intial value of R. namely R_a, is determined for attenuation A due to debris rain and used to obtain a value for W_d. Adjustments in W_c, R_i, W_d, and R_a are then likely to be required.

For example, W_c is replaced by W_c' = Min of W_c and D_c, and W_d is replaced by W_d' = Min of W_d and D_d. Additionally if $W_c' > W_T$, where W_T is based on modeling Of thickness, W_c' is reduced to $W_c'' = W_T$, , and if $W_d' > W_L$, "d"s reduced to "d" = "L, where W_L is based on thickness modeling. Also if $W_c < D_c$ a contribution C of debris rain is added to the effect of the rain cell so that whereas

$$R_i = \frac{0.7\ A \cos\theta}{1.87\ a} \left[\frac{1}{} \right]^{1/(b\ -0.04)} \qquad \text{(A4.10)}$$

$$\text{"f} = \left(\frac{C\ A\ \cos\theta}{W_c'\ a} \right)^{1/b} \qquad \text{(A4. 11)}$$

The parameters a and b are those of $\alpha = a R^b$ with R the rain rate.

The probability P_f of the path intersecting a rain cell is found from

$$\text{"f} = P_c (1 + De/We") e^{-R_f/R_c} \qquad \text{(A4.12)}$$

where P_c and R_c are from tables provided and apply to the particular rain-rote region in question. The probability of inrersecting debris is

$$P_g = P_d (1 + D_d/W_d'') \frac{1}{2} \operatorname{erfc} \left(\frac{\ln ((\bar{R}_z/\bar{R}_{dl}))}{2^{1/2}\ S_d} \right) \qquad \text{(A4.13)}$$

where P_c, R_d, and S_d are from tables and R_z "s "he final value "f " debris rain rate. The parameters W_c'' and W_d'' are the final values of what were originally designated as W_c and W_d. Finally the total probability P of attenuation greater than A_{dB} is given by

$$P = P_f + P_g \qquad \text{(A4.14)}$$